Fault-Tolerant Unfalsified Control for PEM Fuel Cell Systems

Fernando D. Bianchi, Carlos Ocampo-Martinez*, Senior Member, IEEE*, Cristian Kunusch*, Member, IEEE*, and Ricardo S. Sánchez-Peña*, Senior Member, IEEE*

***Abstract*—This paper addresses the implementation of a data-driven control strategy in a real test bench based on proton exchange membrane fuel cells (PEMFCs). The proposed control scheme is based on unfalsified control, which allows adapting in real time the control law by evaluating the performance specifications based only on measured input–output data. This approach is especially suitable to deal with nonlinearity, model uncertainty, and also possible faults that may occur in PEMFCs. The control strategy has been applied to several experimental practical situations in order to evaluate not only the system performance, but also different fault scenarios. The experimental results have shown the effectiveness of the proposed approach to regulate the oxygen stoichiometry in real-time operation, as well as to maintain a proper system performance under fault situations. Also, a start-up mass-flow controller is added in order to bring the system toward its normal operating conditions.**

Q1

***Index Terms*—Fault-tolerant control (FTC) tests, oxygen stoichiometry, polymer electrolyte membrane fuel cells (PEMFCs), unfalsified control (UC).**

I. Introduction

THE EVOLUTION of modern society has been mostly based on the consumption of fossil fuel for electricity
Q2 generation and the functioning of critical infrastructures such as transport networks. This model is strongly dependent on the constantly decreasing reserves of that type of fuel, which is also related to hazardous problems such as global warming. However, there are several options for electricity generation beyond fossil fuels that could mitigate the dependence modern society has with these scarce and polluting resources. Clean energy sources and, in particular, fuel cells (FCs) as electrochemical devices that generate electrical energy from hydrogen and oxygen, with pure water and heat as byproducts, are regarded as one of the most promising technologies due to their potential efficiency, compactness, and reliability [1]. Important advances in the design of these devices as well as on their materials allow to consider FCs viable for electricity generation not only at small scale (automotive), but also as technologies embedded in complex arrays of polygeneration such as the so-called smart energy grids [2]. In particular, polymer electrolyte membrane FCs (PEMFCs) are a type of FCs especially developed for both portable and stationary applications. Their distinguished features include lower pressure ranges, temperatures from 45 to $95\,^{\circ}\mathrm{C}$ and a special polymer electrolyte membrane (conducting hydrogen protons) [3].

Despite the notorious advantages of these devices and the widespread availability of hydrogen as a fuel, several technological challenges related to the PEMFC efficiency, lifetime, and economical costs are still open as major limitations for their standard implementation in everyday solutions. This fact, together with the recent advances in material sciences and component enhancements, makes advanced control techniques appear as complementary strategies in order to reduce costs, improve performance, and optimize efficiency, therefore increasing the lifetime of PEMFC-based systems. Hence, reliable control systems may ensure system stability and performance, as well as robustness against uncertainties and exogenous perturbations, all properties of capital importance for PEMFC success. Several research works have addressed the oxygen stoichiometry control to optimize the system conversion efficiency, avoiding performance deterioration together with eventual irreversible damages in the polymeric membranes due to oxygen starvation. These works present the way to achieve the aforementioned control objective by using different techniques: model predictive control (MPC) [4], sliding-mode control [5], full-state feedback
with integral control [6] or LQR/LQG-based control [7], linear Q5
parameter varying control [8], and adaptive control [9], among others.

One important aspect when controlling real systems is concerned with the occurrence of component faults and their influence in the overall system performance. In fact, faults and model/sensor/actuator uncertainty play similar roles, then the conceptual distinction among them represents the difference between *active*[1] and *passive*[2] fault-tolerant control (FTC)

Manuscript received February 15, 2014; revised July 7, 2014; accepted August 13, 2014. The work of C. Ocampo-Martinez and C. Kunusch was supported by the Project MACPERCON (Ref. 201250E027) of the CSIC. The work of
Q3 C. Kunusch was supported by the seventh Framework Programme of the European Union through the Marie Curie actions (GA: PCIG09-GA-2011-293876) and the Puma-Mind Project (GA: FCH-JU-2011-1-303419), as well as by the CICYT Project DPI2011-25649 (MICINN-Spain). The work of R. S. Sánchez
Q4 Peña was supported by CONICET and Grant PICT2008-290 from the PRH Program of the Ministry of Science, Technology, and Innovation of Argentina. Paper no. TEC-00097-2014.

F. D. Bianchi is with the Department of Electrical Engineering, Catalonia Institute for Energy Research, 08930 Barcelona, Spain (e-mail: fbianchi@irec.cat).

C. Ocampo-Martinez and C. Kunusch are with Institut de Robtica i Informtica Industrial, Universitat Politècnica de Catalunya, 08028 Barcelona, Spain (e-mail: cocampo@iri.upc.edu; ckunusch@iri.upc.edu).

R. S. Sánchez-Peña is with CONICET and the Instituto Tecnológico de Buenos Aires, C1106ACD Buenos Aires, Argentina (e-mail: rsanchez@itba.edu.ar).

Color versions of one or more of the figures in this paper are available online at http://ieeexplore.ieee.org.

Digital Object Identifier 10.1109/TEC.2014.2351838

[1]Active FTC strategies aim at adapting the control loop based on the information provided by an FDI module within the fault-tolerant architecture.

[2]In passive FTC strategies, a single-control law is used in both faultless and faulty operation, assuming a certain degree of performance degradation.

design approaches [10]. In the framework of FCs and assuming an active FTC architecture, several approaches for fault detection and isolation (FDI) have been proposed. Model-based FDI for PEMFC systems based on consistency relations for the detection and isolation of predefined faults has been proposed in [11], while in [12], a comparison of both model-based and data-driven fault detection methods for FCs is addressed. The work in [13] proposes a methodology to use the electrical model for FC system diagnosis, while in [14], a fault diagnosis and accommodation system based on fuzzy logic has been developed as an effective complement for a closed-loop scheme. Regarding FTC, Xu *et al.* [15] present an experimental implementation of an active FTC system for an FC/battery hybrid power train applied to a city bus, while Feroldi [16] proposes an MPC scheme for adding fault tolerance capabilities to a two-actuator PEMFC system.

Unfalsified control (UC) theory was born as an approach for data-driven control, where no prior hypothesis on the plant is used besides the measured data streams [17]. The control law is selected from a predefined set by the performance evaluation based solely on the information provided by the measured input–output (I/O) data. The controllers that do not achieve the desired performance specifications are discarded (falsified). Instead, one of the remaining (unfalsified) controllers is used, until it is falsified by the past measurements and replaced by a new UC and so on. This technique has been formally introduced by Safonov and Tsao [18]. UC is a real-time implementation method that may be combined with other model-based design techniques, hence it is not mutually exclusive [19].

At this point, UC emerges as an especially suitable technique to tackle the complex characteristics inherent to FC systems. Nonlinear dynamics, inaccessible variables, and model uncertainties are natural addresses by UC. Being a data-driven approach, UC is also particularly suited for dealing with unknown disturbances and possible fault occurrences. The application of UC in other systems has been previously reported in the literature and ranges from chemical reactors [20], flight control systems [21], up to microaerial vehicles [22], among others. In [23], the implementation of an ellipsoidal UC (EUC) in a dual rotary fourth-order motion system is presented, showing the success of the experimentation by ensuring the convergence of the proposed algorithm. By a suitable selection of the controller set and the performance test, EUC is capable of an efficient implementation of UC ideas as a convex optimization problem easily implemented in real time. From the best of the author's knowledge, UC has never been implemented in the control/supervision of a complex system based on PEMFCs.

The main contribution of this paper is a robust oxygen stoichiometry control design based on UC and its implementation in a laboratory FC system. In particular, an EUC-based closed-loop scheme [24] is designed and tested experimentally under several scenarios. The control objectives cover the traditional stoichiometry regulation, disturbance rejection represented by changes in the load profile of the PEMFC, and also the consideration of actual fault events in the components, which may induce performance loss and hazardous operation of the entire system. The proposed approach may be integrated into a multilevel supervisory control scheme, where other system variables might be simultaneously regulated toward the improvement of global objectives such as durability and efficiency of the overall PEMFC system [25]. Experimental results have shown the effectiveness of the proposed approach in fulfilling the control objective (stoichiometry regulation) in real-time system operation. The overall scheme proposed in this paper also includes a start-up mass-flow control strategy, which avoids an abrupt/nonsmooth behavior of the system variables when the EUC controller is started with initial conditions far away from the nominal system operation. The scheme proposed in this paper introduces fault tolerance capabilities as in [26], but considering the proposed fault scenarios over the real experiment.

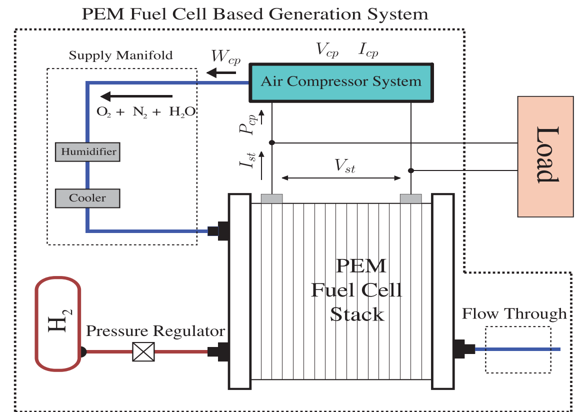

Fig. 1. Schematic diagram of the PEMFC-based generation system.

The remainder of this paper is organized as follows. Section II briefly describes the physical system and control objectives as well as the main parts of the experimental test bench. Section III introduces the EUC techniques as well as the necessary modifications in order to implement it in the real case presented here. Section IV collects and explains in detail the experimental results for different practical scenarios, and Section V presents the main conclusions.

II. System Physical Description

The system is comprised by a central PEMFC stack and additional/complementary units. In Fig. 1, the scheme of the considered system and the interaction between its different subsystems (FC stack, reactant supply system, and humidity management unit) is shown. A brief description of some components, variables, and processes is presented as follows. In the system, the control input u corresponds to the compressor voltage denoted $V_{\rm cp}$. The system output y corresponds in turn to the inlet stoichiometry of the PEMFC cathode, namely λ_{O_2}. Moreover, the system is affected by the external disturbance $I_{\rm st}$, which corresponds to the stack current flowing toward the load.

The main subsystems depicted in Fig. 1 are as follows:

1) a 12-V dc air compressor with an oil-free diaphragm vacuum pump, whose input voltage $V_{\rm cp}$ is the control variable (as established beforehand);
2) hydrogen and oxygen cellkraft membrane exchange humidifiers and line heaters, which are used to maintain

proper humidity and temperature conditions inside the cell stack[3];

3) a ZBT 8 fuell-cell stack with Nafion 115 membrane electrode assemblies with 50 cm^2 of active area and 150-W power.

Moreover, different sensors are incorporated into the system such as an air-mass flowmeter (range 0–15 slpm) at the end of the compressor to measure its flow ($W_{\rm cp}$), a current clamp (range 0–3 A) and a voltage meter (range 0–15 V) to measure the motor stator current ($I_{\rm cp}$) and voltage ($V_{\rm cp}$), respectively. Besides, temperature sensors are arranged in order to register the different operation conditions. The full description of this system, as well as a fully validated nonlinear dynamic model specially developed for control purposes are presented and deeply discussed in [3]. Given the complexity of the nonlinear model and the consequent difficulty for designing and implementing online controllers, data-driven control techniques rise as an attractive alternative for real-time operation of such systems, mainly when different experimental scenarios are considered.

In order to maximize the efficiency of the PEMFC system, the regulation of the oxygen mass inflow toward the stack cathode should be achieved. Additionally, oxygen starvation and irreversible membrane damage are averted. To accomplish such an oxidant flow is equivalent to maintaining the oxygen excess ratio of the cathode at a suitable value. The oxygen excess ratio or oxygen stoichiometry is defined as

$$\lambda_{O_2} = \frac{W_{O_2,\rm ca}}{W_{O_2,\rm react}} \tag{1}$$

where $W_{O_2,\rm react}$ is the oxygen flow consumed in the reaction and $W_{O_2,\rm ca}$ is the oxygen partial flow entering the cathode, which depends on the air flow released by the compressor $W_{\rm cp}$, i.e.,

$$W_{O_2,\rm ca} = \frac{\chi_{O_2} W_{\rm cp}}{1+\omega_{\rm amb}}. \tag{2}$$

Here, $\omega_{\rm amb}$ is the ambient air humidity ratio and χ_{O_2} is the molar fraction of oxygen in the air ($\chi_{O_2} = 0.21$). As $W_{O_2,\rm ca}$ is an internal unavailable variable of the system, it is not practical to include it in the control algorithm. This problem was circumvented by inferring information of $W_{O_2,\rm ca}$ from an accessible variable of the system, such as the air-mass flow delivered by the compressor

$$\begin{aligned} W_{\rm cp} = \; & B_{00} + B_{01}\omega_{\rm cp} + B_{02}\omega_{\rm cp}^2 \\ & + (B_{10} + B_{01}\omega_{\rm cp})\Psi + B_{02}\Psi^2 \end{aligned}$$

being $\Psi = m_{a,\rm hum} T_{\rm hum} R_a / V_{\rm hum} + K_{\rm hum}$, $\omega_{\rm cp}$ is the compressor speed, and $m_{a,\rm hum}$ is the humidifier mass of air. The compressor parameters B_{00}, B_{01}, B_{10}, B_{11}, B_{02}, and B_{20} can be obtained from [5], $T_{\rm hum}$ is the humidifier temperature, $V_{\rm hum}$ is the humidifier volume, R_a is the air gas constant, and $K_{\rm hum} = P_{\rm sat}(T_{\rm hum}) RH_{\rm hum} - P_{\rm sat}(T_{\rm amb}) RH_{\rm amb}$, with $P_{\rm sat}(T_{\rm hum})$ being the vapur saturation pressure at $T_{\rm hum}$, $RH_{\rm hum}$ the relative humidity of the gas at the humidifier output, $P_{\rm sat}(T_{\rm amb})$ the vapur saturation pressure at ambient temperature, and $RH_{\rm hum}$ the relative humidity of ambient air.

Note that $W_{O_2,\rm react}$ is directly related to the stack current as follows:

$$W_{O_2,\rm react} = G_{O_2} n I_{st} / 4F \tag{3}$$

with G_{O_2} is the molar mass of oxygen, n is the number of cells, and F is the Faraday's constant. As presented in the validated model [3], the operating conditions of the system inputs are determined by $V_{\rm cp}$ and $I_{\rm st}$.

This paper is focused on the oxygen stoichiometry λ_{O_2} tracking under continuous changes in the load condition $I_{\rm st}$, such that

$$e_\lambda = \lambda_{O_2} - \lambda_{O_2,\rm ref} \tag{4}$$

is as small as possible for both nominal and fault conditions. In (4), $\lambda_{O_2,\rm ref}$ corresponds to a given reference value, which comes from a supervisory controller that considers global objectives related to the efficiency and durability of the overall PEMFC-based system [25].

III. UC OF PEMFCs

The UC concept proposed by [18] consists of a set of candidate controllers $\mathbf{K}$ and a switching algorithm that selects the most suitable controller in the set according to a performance criterion based only on experimental I/O data. The main appeal of UC is that there is no need of a plant model to decide if a controller satisfies the performance specifications.

The only *a priori* information needed about the system is a set of I/O measures $\mathcal{Z}(k) = \{(u(l), y(l)), 0 \le l \le k\}$, with k being the discrete time. The performance specifications are stated as a cost-function $\mathcal{V}$ depending on the reference r, and on the input u and output y. As a consequence, the performance specifications define a subset

$$\mathcal{T}_{\rm spec} = \{(r, u, y) : \mathcal{V}(r, u, y) < \eta\}$$

where η is a positive scalar bounding the performance specifications. In turn, a candidate controller $K \in \mathbf{K}$ also defines a subset

$$\mathcal{K} = \{(r, u, y) \; : \; u = K(r, y)\}$$

where K must be "causally-left-invertible," i.e., there exists K^{-1} that allows the computation of a fictitious reference r_f from (u, y). This reference is the value that r would take if the controller K is inserted in the loop, and the I/O of the plant were (u, y). The fictitious reference can be computed from $\mathcal{Z}$ and K, without actually inserting the controller in the loop, as follows:

$$r_f = K^{-1}(u, y). \tag{5}$$

In this framework, the controller K is said to be unfalsified by the experimental information $\mathcal{Z}$ if

$$\mathcal{K} \cap \mathcal{Z} \cap \mathcal{T}_{\rm spec} \neq \emptyset \tag{6}$$

otherwise the controller is said to be falsified by the measured data. The problem is feasible if the set of candidate controllers

[3]Decentralized PID controllers are in charge of ensuring the adequate operation values for these devices; therefore, this control design is out of the scope of this paper.

includes at least one which stabilizes the system (see [19, p. 18]).

The selection of the most adequate controller, also denoted the falsification procedure, according to the *a posteriori* information (u, y) relies on the evaluation of a cost-detectable function. This property guarantees stability and convergence of the adaptive procedure.

The controller set may have a finite or infinite number of controllers. In the first case, all the controllers in the set are tested simultaneously. That could be computationally demanding if it contains a large number of controllers. In the second approach, the set is defined by a control structure that updates its parameters in real time. The selection of the most suitable controller relies on an optimization procedure that computes the best controller parameters. This option could be more computationally efficient but is limited to certain cost functions. Hence, the proper selection of these cost functions is done in such a way that the controller selection results in a convex optimization easy to solve online. The UC technique used here is based on this latter approach.

A. Ellipsoid Unfalsified Control

The cost function and the controller structure define the falsifier complexity. In particular, the EUC, by selecting an adequate cost function and a certain control structure, computes the most suitable controller by means of an efficient convex optimization procedure and with proven convergence properties [24]. Most precisely, the controllers are parameterized as

$$u(k) = \begin{bmatrix} r(k) \\ \Lambda_u(z^{-1})u(k) \\ y(k) \\ \Lambda_y(z^{-1})y(k) \end{bmatrix}^T \begin{bmatrix} 1/\hat{\theta}_1 \\ -\hat{\theta}_2/\hat{\theta}_1 \\ -\hat{\theta}_3/\hat{\theta}_1 \\ -\hat{\theta}_4/\hat{\theta}_1 \end{bmatrix} \quad (7)$$

where Λ_u and Λ_y are stable linear filters, $\hat{\theta}_i$ $(i = 1, \ldots, 4)$ are parameters to be set online, and z is the unity delay. With this parameterization, the fictitious reference can be found as

$$r_f(k) = w^T(u, y, k)\theta \quad (8)$$

where

$$w = \begin{bmatrix} u(k) \\ \Lambda_u(z^{-1})u(k) \\ y(k) \\ \Lambda_y(z^{-1})y(k) \end{bmatrix}, \quad \theta = \begin{bmatrix} \theta_1 \\ \theta_2 \\ \theta_3 \\ \theta_4 \end{bmatrix}.$$

The controller parameterization and the computation of the fictitious references are illustrated in Fig. 2. Note the difference between the parameter $\hat{\theta}$ of the current controller and the parameter θ under performance evaluation by the UC algorithm.

The performance criterion is cast in the form of model reference tracking as

$$|e_f(\theta, k)| + \kappa|u(k)| \leq \Delta(k) \quad (9)$$

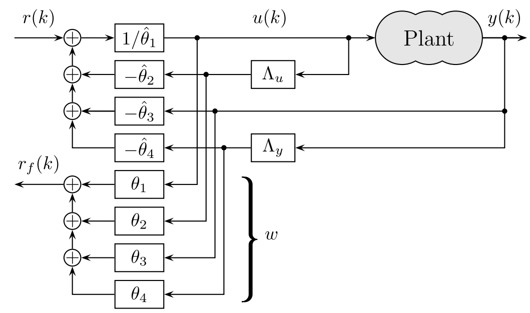

Fig. 2. Controller parameterization and fictitious reference computation.

where $e_f(k) = G_m(z^{-1})r_f(\theta, k) - y(k)$, G_m is a stable system that defines the desired behavior, and $\Delta(\cdot)$ is a time-dependent bound. Then, the set of controller parameters that satisfy the performance specifications is given by

$$\mathcal{U}(k) = \{\theta \,:\, -\hat{\Delta}(k) \leq e_f(\theta, k) \leq \hat{\Delta}(k)\} \quad (10)$$

where $\hat{\Delta}(k) = \Delta(k) - \kappa|u(k)|$. The set of controllers is given by (7) and the parameter set

$$\mathcal{E}(k) = \{\theta \,:\, (\theta(k) - \theta_c(k))^T \Sigma(k)(\theta(k) - \theta_c(k))\} \quad (11)$$

where $\mathcal{E}(k)$ is an ellipsoid of center $\theta_c(k)$ and size is defined by the positive-definite matrix $\Sigma(k)$ [24].

With these definitions, the controller and specification sets are parameterized in θ and condition (6) results in

$$\mathcal{E}(k) \bigcap \mathcal{U}(k) \neq \emptyset. \quad (12)$$

That is, the set of UCs is given by the parameters θ in the intersection of $\mathcal{E}(k)$ and $\mathcal{U}(k)$. Therefore, the falsification algorithm reduces to shrinking the ellipsoid volume (vol($\mathcal{E}(k)$)) by changing the matrix $\Sigma(k)$, to check the intersection of $\mathcal{E}(k)$ and $\mathcal{U}(k)$, and to select a new $\hat{\theta} \in \{\mathcal{E}(k) \bigcap \mathcal{U}(k)\}$.

The original EUC algorithm was intended for time-invariant systems and the volume of the ellipsoid was reduced as long as the *a posteriori* information increased, and thus, the controller parameters converged to the controller that satisfied the performance specifications. In other words, when the number of samples of (u, y) increases, the information is used to remove those controllers that do not satisfy the performance criterion. In case of time-varying or nonlinear systems, a controller falsified for certain operating conditions could satisfy the performance criterion in other operating points. Therefore, the EUC algorithm needs some modification in order to cover these cases. Here, the expansion of the ellipsoidal volume, when no controller is falsified, is proposed. More precisely, if the current controller parameter are not falsified after k_{th} samples, the ellipsoid volume vol($\mathcal{E}(k)$) is expanded by changing the matrix Σ as follows:

$$\Sigma(k+1) = \Sigma(k)\beta^p$$

where $\beta > 1$ and p increases by 1, each time the current controller remains unfalsified during more than k_{th} samples. The expansion continues until the controller is falsified or the initial volume is reached.

B. EUC for PEMFC

To design an EUC control algorithm it is necessary to choose the filters Λ_u and Λ_y, which define the controller set and the transfer function G_m to define the desired behavior. Although EUC does not require *a priori* information of the plant, it is always useful to have a rough idea about its dynamics and the structure needed to achieve the desired closed-loop behavior.

In the case of the PEMFC, the system behavior around an operating point can be roughly approximated by a second-order system of the form

$$G(z) = \frac{\lambda_{O_2}(z)}{V_{\text{cp}}(z)} = K_{fc}\frac{z-a}{(z-b)(z-c)}. \qquad (13)$$

By selecting

$$\Lambda_u(z) = \Lambda_y(z) = \frac{K_\Lambda}{z-q} \qquad (14)$$

and the control law

$$u(k) = \frac{1}{\theta_1}r(k) - \frac{\theta_2}{\theta_1}\cdot\frac{K_\Lambda}{z-q}u(k) - \left(\frac{\theta_3}{\theta_1} + \frac{\theta_4}{\theta_1}\cdot\frac{K_\Lambda}{z-q}\right)y(k) \qquad (15)$$

and for the particular values $\theta_3 = 1$ and $\theta_4 = 0$, the controller results

$$u(k) = \frac{1}{\theta_1}\cdot\frac{z-q}{z-(q-\theta_2 K_\Lambda/\theta_1)}(r(k)-y(k)). \qquad (16)$$

With proper values of θ_1 and θ_2, it is possible to obtain a closed-loop transfer function of the form

$$G_{cl}(z) = \frac{\lambda_{O_2}(z)}{\lambda_{O_2,\text{ref}}(z)} = \frac{K_{cl}}{z-q_{cl}}. \qquad (17)$$

Therefore, it is reasonable that the desired closed-loop behavior given by G_m has the form of G_{cl} in (17).

IV. Experimental Results

This section describes the different scenarios considered for testing the effectiveness of the proposed control approach. For every scenario, the main results are discussed through the most relevant variables involved in each case. They include typical performance tests and the effect of faults in different parts of the PEMFC-based system. Before analyzing the experimental results, a brief description of the experimental test bench and the particular EUC settings are presented.

A. Workplace Setup

The control strategy was implemented in a complete data acquisition and control system. It is composed of two computers (each with four i5 core processors at 2.6-GHz clock frequency): the host and the real-time operating system. The former provides the software development environment and the graphical user interface. It is responsible for the startup, shutdown, configuration changes, and control settings during operation. The latter implements the control algorithms and the data acquisition via a field-programmable gate array in order to have high-speed data processing. Control, security, and monitoring tasks are conducted by a CompactRIO (reconfigurable I/O) system from National Instruments. In order to record the analog sensor signals, a 32-channel 16-bit analog input module from National Instruments is used (NI-9205). An eight-channel, digital I/O module generates the necessary transistor–transistor logic signals for different security and diagnostic tools. Fig. 3 shows the laboratory setup used in the experiments.

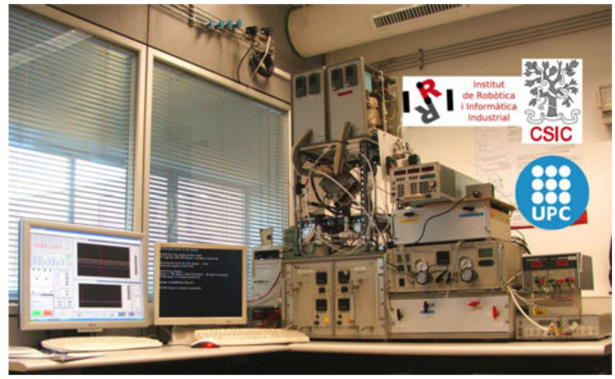

Fig. 3. Picture of the laboratory test station at IRI (CSIC-UPC).

B. EUC Controller Setup

The EUC algorithm has been developed in MATLAB and then crosscompiled into a LabView environment by means of a *DLL* file obtained through the MATLAB real-time workshop toolbox.

The tracking error was bounded with the function

$$\Delta(k) = 0.25 + 1.9e^{-0.02k}$$

which ensures a 2% tracking error and relaxes the error during the initial transients, avoiding excessive controller falsifications.

The filters were selected as

$$\Delta_y(z) = \Delta_u(z) = \frac{0.00897}{z-0.991}$$

and the reference model as

$$G_m(z) = \frac{0.0198}{z-0.9802}.$$

These transfer functions were selected based on linear models identified at several operating points; therefore, the adopted control structure allows achieving the desired closed-loop behavior. The sampling time was 0.01 s.

The initial value of the controller parameters was

$$\theta_0 = \begin{bmatrix}2 & -1.99 & 1 & 0\end{bmatrix}^T.$$

The parameters for the expansion of the ellipsoid volume were set as $\beta = 1.5$ and $k_{\text{th}} = 100$.

C. Complete Control Strategy

The UC is complemented with a bumpless and a flow control to help in the startup of the system. This complementary start-up controller acts as a safety strategy to avoid undesired consequences in the FC stack durability, regulating the air-mass inflow from the compressor. Thus, W_{cp} is regulated toward a convenient value in such a way that λ_{O_2} reaches values close

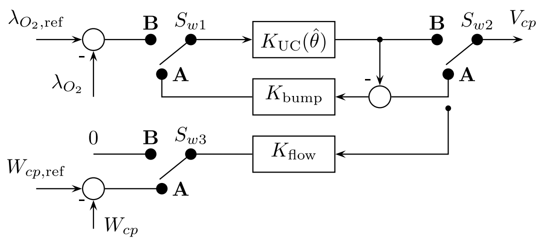

Fig. 4. Complete control scheme including the UC and the start-up controllers.

to its desired reference $\lambda_{O_2,\text{ref}}$ [given that both variables W_{cp} and λ_{O_2} are related by means of (1) and (2)]. Therefore, a smooth starting behavior of λ_{O_2} is achieved. The complete control scheme is sketched in Fig. 4.

In this initial stage, the switches $S_{w1} = S_{w2} = S_{w3}$ are set at position **A** and the controller

$$K_{\text{flow}}(z) = 0.43 + \frac{0.043}{z-1}$$

tracks a predefined profile leading the system to a suitable flow condition before starting the stoichiometry control. This PI controller was designed experimentally based on the step response of the system under the initial operating conditions to ensure a settling time lower than 1 s.

The bumpless controller

$$K_{\text{bump}}(z) = 0.3175 + \frac{0.2}{z-1}$$

ensures a smooth transition from flow to stoichiometry control. This PI controller was designed to ensure that $K_{\text{UC}}(\theta_0)$ achieves a rapid tracking of the signal V_{cp} produced by K_{flow}.

Once a preset time is reached, the $S_{w1} = S_{w2} = S_{w3}$ are set at position **B** and the control switches to stoichiometry control. Initially, the EUC starts with a fixed initial control given by θ_0. This can be a conservative controller that covers the complete operating envelope in a stable way, but with poor performance. Once the EUC is fully operative, the switching algorithm is responsible for finding a more suitable parameter θ to achieve a better performance in the actual operating conditions.

D. Experimental Scenarios

In order to evaluate the performance of the proposed closed-loop control scheme, the following realistic scenarios are considered for covering not only nominal (faultless) situations, but also the effect of real faults in the system. Note that these tests include a real set of safety measures and devices that avoid any hazardous behavior of the test bench (like over pressures, temperatures, or currents). The anode line is also monitored by a higher level supervisor, avoiding any irreversible damages in the cells due to high-differential pressure between anode and cathode.

1) Scenario 1 (Start-up Controller and Reference Tracking): This scenario considers two parts; the system behaviour with a start-up flow controller and the reference tracking performance. First of all, in order to carry the system variables toward an initial operation regime, the overall control structure considers the initial regulation of the compressor flow W_{cp} at a given value,

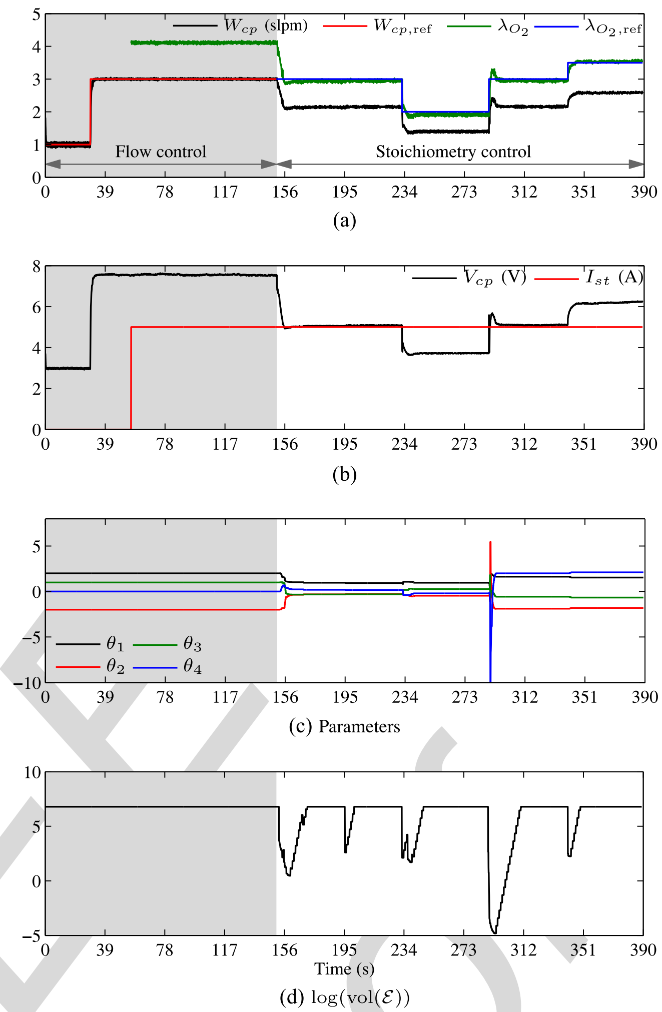

Fig. 5. Start-up and closed-loop response for several step changes in the stoichiometry reference (Scenario 1).

close enough to nominal operating points when the stack is delivering electrical power. In this initial stage, the falsification algorithm is out of the loop and will only be activated after W_{cp} reaches its reference value

$$W_{\text{cp, ref}} = (1 + \omega_{\text{atm}})\lambda_{o2,\text{ref}} G_{O_2} n I_{\text{st}}/(4F\chi_{o2}).$$

Fig. 5 presents the behaviour of the system variables for this scenario. Note that the stoichiometry is not well defined, until I_{st} is greater than zero. Q6

After 150 s of flow regulation, the closed-loop system switches to an initial stabilizing controller ($\theta = \theta_0$) before activating the EUC controller at time $t = 152$ s [see the transitions in the ellipsoid volume parameter $\text{vol}(\mathcal{E}(k))$ in Fig. 5(d)] and considers different values for the oxygen stoichiometry reference $\lambda_{O_2,\text{ref}}$ ranging from 2 to 3.5. Here, the stack current I_{st} remains constant at 5 A. This is a typical scenario where the oxygen stoichiometry of a PEMFC-based system is changed to obtain different net powers. Although the flow control is no longer connected, W_{cp} follows the stoichiometry evolution due to their relation given by (1) and (2). Once the EUC is activated, notice the suitable change of parameters θ_i in Fig. 5(c), which

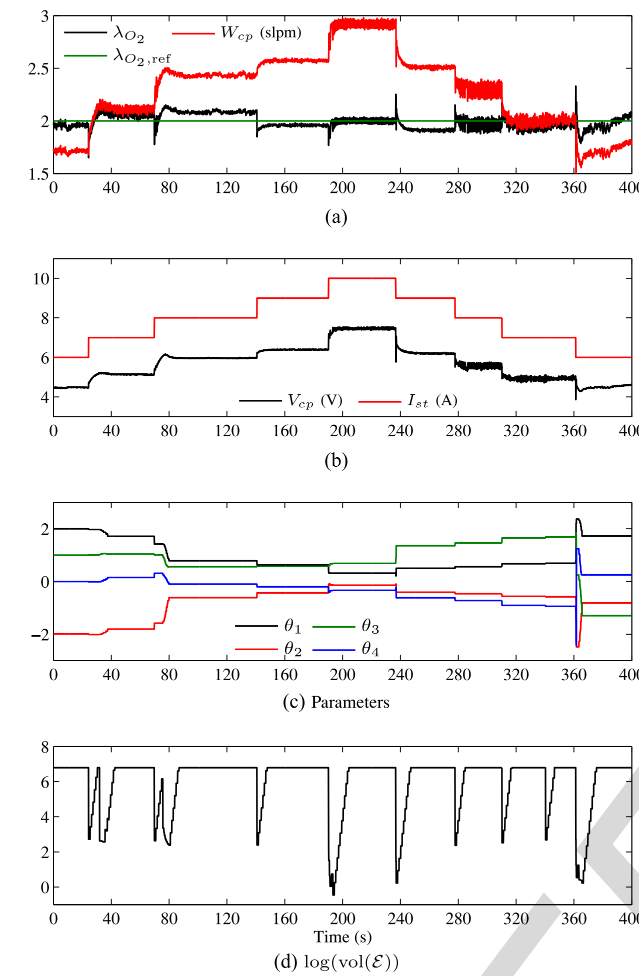

Fig. 6. Closed-loop response for several step changes in I_{st} (Scenario 2).

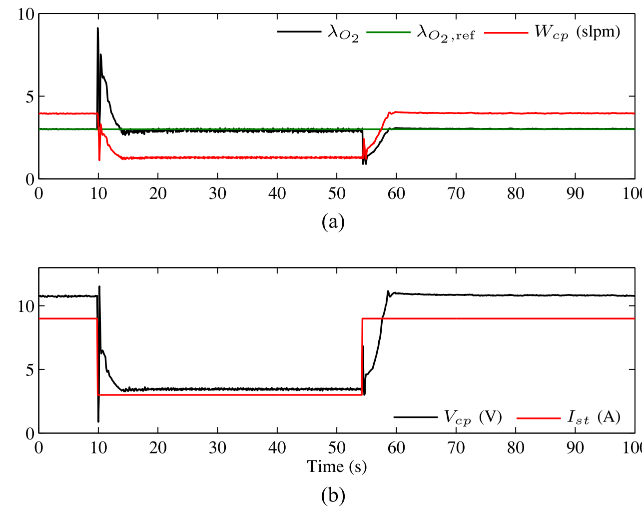

Fig. 7. Closed-loop response for 6 A step changes in I_{st} (Scenario 2).

induces smooth changes in the control signal V_{cp} [see Fig. 5(b)] in order to adapt the controller to different operating conditions associated with the different values of $\lambda_{O_2,\mathrm{ref}}$. This reference can be directly computed offline or through an extremum seeking algorithm like the one presented in [25], where the goal is to optimize the overall system efficiency. The bottom plot shows the evolution of the ellipsoid volume $\mathrm{vol}(\mathcal{E}(k))$ (in logarithmic scale). It can be seen that after $k_{\mathrm{th}} = 100$ samples without any controller falsification, the algorithm expands the volume to be better prepared for new operating conditions.

2) Scenario 2 (Disturbance Rejection): Considering that the desired value of $\lambda_{O_2,\mathrm{ref}}$ is already reached, it is also important to evaluate the performance of the EUC-based closed-loop system when changes in the load current I_{st} take place. To reproduce this typical working case, $\lambda_{O_2,\mathrm{ref}}$ was set at 2, while different values of I_{st} have been required from the PEMFC stack. Fig. 6 shows the main variables related to this test. Note that λ_{O_2} is rapidly reaching the new steady state desired value after each change of I_{st}. Meanwhile, the parameters θ_i are being adapted to this end [see Fig. 6(c)], with changes in I_{st} between 6 and 10 A and smooth changes of the control signal V_{cp}. The lower plots shows the updates of the controller parameters and the changes in the ellipsoid volume $\mathrm{vol}(\mathcal{E}(k))$, when the operating conditions change as a consequence of changes in I_{st}. It can be seen that parameters θ_i change more than once for constant values of I_{st}. This is mainly a consequence of the noise in the measures of V_{cp}.

Besides, Fig. 7 shows the stoichiometry regulation under a demanding scenario, in which the current I_{st} increases and decreases in step changes of 6 A. Even under demanding conditions, the proposed EUC control scheme is capable of rapidly returning the stoichiometry to the set-point value. To properly handle these abrupt step changes, faster devices such as supercapacitors and/or batteries should be connected in parallel with the PEMFC system.

3) Scenario 3 (Cathode Outflow Fault): This scenario considers the effect of a couple of faults in the performance of the PEMFC-based system. Faults in this case are related to the cathode outflow in the following way 1) there is a flow blockage (FB) that causes the increase of the cathode inlet pressure P_{ca}, and 2) there is a flow leak (FL) that is compensated by increasing V_{cp} without affecting P_{ca}. The goal is to check the behavior of the EUC-based closed loop when rejecting these changes in the cathode line, while both I_{st} and λ_{O_2} remain constant at 5 A and 3, respectively, along the whole experiment. Fig. 8 shows the system variables related to this test. The magnitude of the FB fault can be quantified by either analyzing the behavior of P_{ca} [see Fig. 8(b)], or computing the compressor power by means of V_{cp} and I_{cp}, both plotted in the same figure. Since the FB fault appearing at $t = 35$ s progressively increases P_{ca}, the EUC controller suitably adapts the parameters during that effect (see transitions of $\mathrm{vol}(\mathcal{E}(k))$ after 35 s). In the case of the FL fault, its magnitude can be quantified by observing V_{cp}, since P_{ca} is not affected due to the compensation performed by the manipulated input after $t = 255$ s. It should be noticed that the proposed control scheme is capable to properly reject the effect of the considered faults, and after a slight deviation, λ_{O_2} returns to its desired reference value. The controller also allows to recover the system even when the fault disappears and the nominal behavior is recovered.

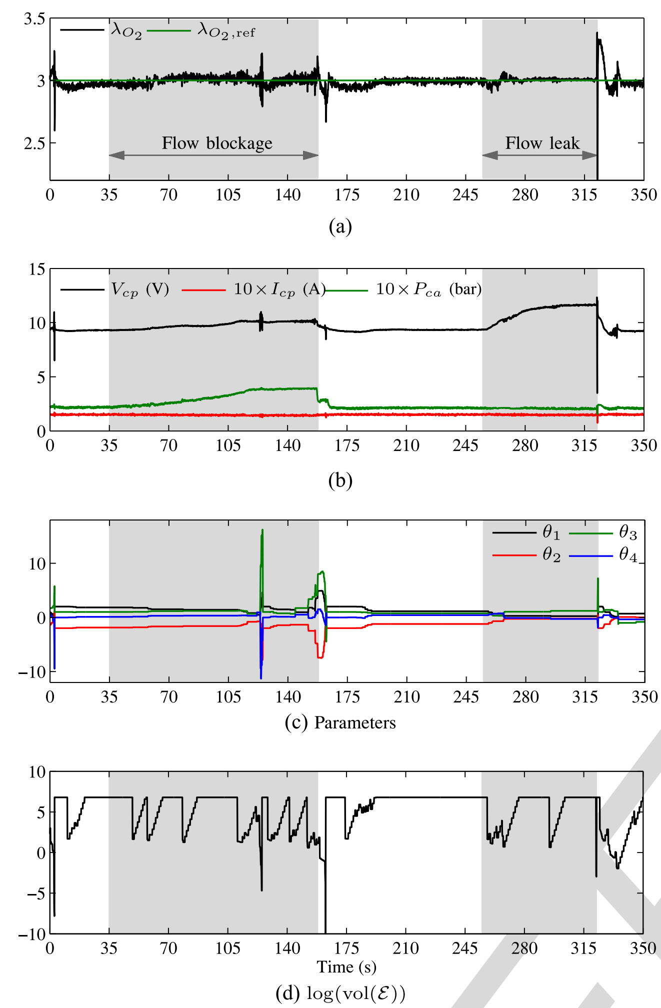

Fig. 8. Closed-loop response during FB and FL faults (Scenario 3).

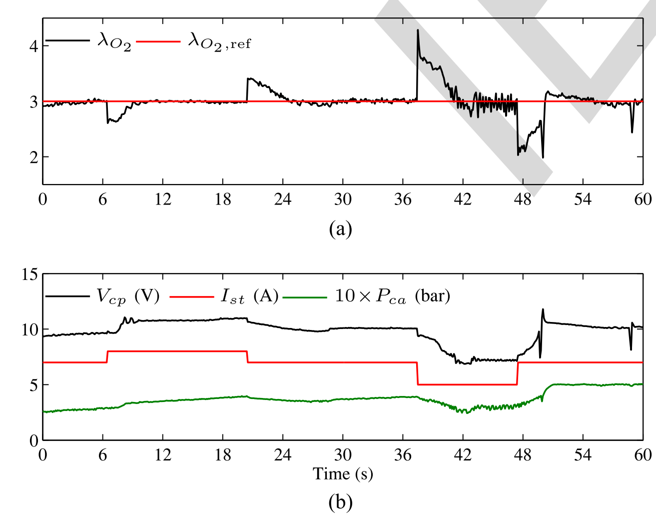

Fig. 9. Closed-loop response for I_{st} changes under an FB fault (Scenario 3).

As an additional evaluation of the proposed control scheme, Fig. 9 shows the disturbance rejection capability under a FB fault. The EUC controller reaches the proper recovery of λ_{O_2}, when several changes of I_{st} were performed.

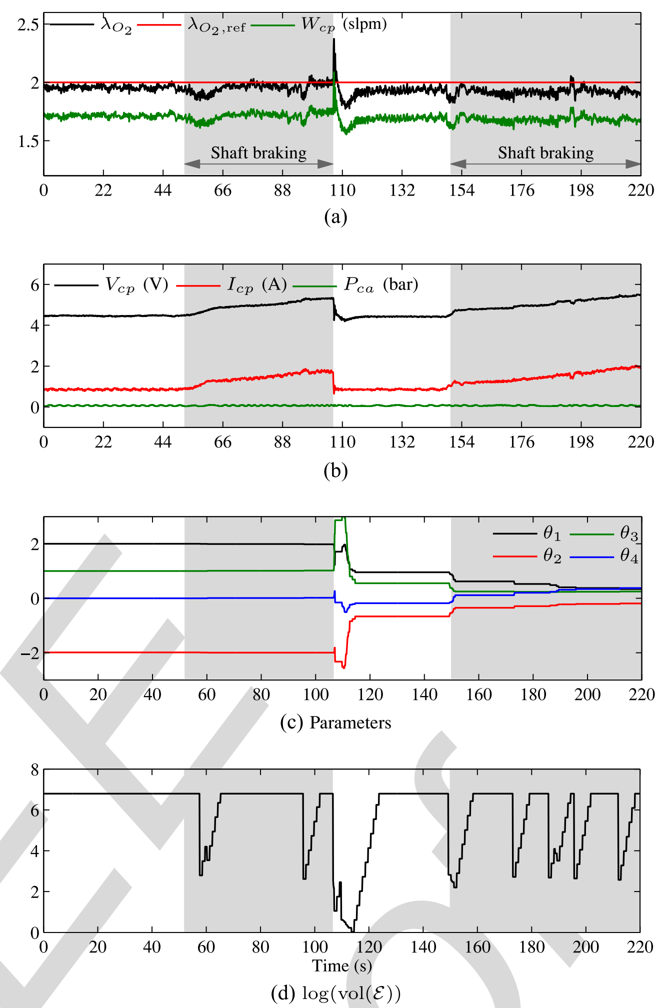

Fig. 10. Closed-loop response during a compressor fault (Scenario 4).

4) Scenario 4 (Compressor Fault): Here, a different fault is considered, which is related to the capacity of the air supply from the compressor connected to the PEMFC cathode. The fault affects the compressor by changing the inertia and nominal friction of its motor shaft. Again, the goal is to check the behavior of the EUC-based closed loop when rejecting this fault, while both I_{st} and λ_{O_2} remain constant at 6 A and 2, respectively. Fig. 10 shows the system variables during this test. The magnitude of the fault in this case is strongly related to I_{cp}, but note that for this case, P_{ca} remains constant [see Fig. 10(b)]. The fault appears at time $t = 50$ s, disappears at $t = 106$ s, and appears again at $t = 146$ s. The EUC controller adapts the parameters θ_i conveniently, while reducing the stoichiometry regulation error as much as possible.

The results presented in this paper mainly highlight the implicit fault tolerance capabilities given by the EUC scheme (due to its data-driven control nature) independently of knowing the particular way the faults affect the system. As stated in the Introduction, several authors have reported the design and implementation of FTC techniques for PEMFC systems, which explicitly use the system model [15], [16] unlike the fault tolerance capabilities of the proposed model-free approach. On the other hand, reported adaptive schemes for PEMFCs address the manipulation of the air-mass flow for controlling λ_{O_2} [8], [27], and the online system identification and efficiency management by controlling λ_{O_2}, relative humidity, and stack temperature [9]. Although those approaches show experimental evidences of their proper operation under nominal conditions, they do not consider the effects of faults over the performance of the closed loop.

V. Conclusion

An FTC for PEMFC was proposed and experimentally tested in a laboratory test bench. The proposed control is based on EUC that allows adapting the controller parameters by evaluating the closed-loop performance solely from measures of the compressor voltage (control input) and the oxygen stoichiometry (controlled output). The EUC algorithm does not rely on a plant model, which makes it suitable for dealing with complex systems and also to tackle faults in the cathode outflow or in the compressor. Four experimental scenarios have shown that the proposed UC control is capable of effectively working in different operating conditions and most common faults in PEMFCs. A start-up mass-flow control strategy has also been introduced, which avoids abrupt changes in the system variables when the initial conditions are far away from the nominal values.

Acknowledgment

All the experimental tests were performed at the PEM Fuel Cells Laboratory, Institut de Robòtica i Informàtica Industrial (CSIC-UPC), Barcelona, Spain, and only possible due to its advanced equipment and proficient technical staff.

References

[1] U.S. Department of Energy, Hydrogen, Fuel Cells and Infrastructure Technologies Program: Multi-Year Research, Development And Demonstration Plan: Planned program activities for 2005–2015. DOE Website. Section 3.4 Fuel Cells, 2005.

[2] J. Blanchard, "Smart energy solutions using fuel cells," in *Proc. IEEE 33rd Int. Telecommun. Energy Conf.*, Amsterdam, The Netherlands, 2011, pp. 1–8.

Q7 [3] C. Kunusch, P. Puleston, M. Mayosky, and A. Husar, "Control oriented modelling and experimental validation of a PEMFC generation system," vol. 6, no. 3, pp. 851–861, 2011.

[4] C. Ziogou, S. Papadopoulou, M. C. Georgiadis, and S. Voutetakis, "Online nonlinear model predictive control of a PEM fuel cellsystem," *J. Process Control*, vol. 23, no. 4, pp. 483–492, 2013.

[5] C. Kunusch, P. Puleston, M. Mayosky, and L. Fridman, "Experimental results applying second order sliding mode control to a PEM fuel cell based system," *Control Eng. Pract.*, vol. 21, no. 5, pp. 719–726, 2013.

[6] J. Pukrushpan, A. Stefanopoulou, and H. Peng, *Control of Fuel Cell Power Systems*. New York, NY, USA: Springer, 2004.

[7] A. Niknezhadi, M. Allué-Fantova, C. Kunusch, and C. Ocampo-Martinez, "Design and implementation of LQR/LQG strategies for oxygen stoichiometry control in PEM fuel cells based systems," *J. Power Sources*, vol. 196, no. 9, pp. 4277–4282, 2011.

[8] F. Bianchi, C. Kunusch, C. Ocampo-Martinez, and R. S. Sánchez-Peña, "A gain-scheduled LPV control for oxygen stoichiometry regulation in PEM fuel cell systems," *IEEE Trans. Control Syst. Technol.*, vol. 22, no. 5, pp. 1837–1844, Sep. 2014.

[9] S. Kelouwani, K. Adegnon, K. Agbossou, and Y. Dube, "Online system identification and adaptive control for PEM fuel cell maximum efficiency tracking," *IEEE Trans. Energy Convers.*, vol. 27, no. 3, pp. 580–592, Sep. 2012.

[10] M. Blanke, M. Kinnaert, J. Lunze, and M. Staroswiecki, *Diagnosis and Fault-Tolerant Control*. Berlin, Germany: Springer-Verlag, 2006.

[11] A. Rosich, R. Sarrate, and F. Nejjari, "On-line model-based fault detection and isolation for PEM fuel cell stack systems," *Appl. Math. Model.*, vol. 38, nos. 11/12, pp. 2744–2757, 2014.

[12] N. Lowery, M. Vahdati, R. Potthast, and W. Holderbaum, "Classification and fault detection methods for fuel cell monitoring and quality control," *J. Fuel Cell Sci. Technol.*, vol. 10, no. 2, pp. 1–8, 2013.

[13] A. Hernandez, D. Hissel, and R. Outbib, "Modeling and fault diagnosis of a polymer electrolyte fuel cell using electrical equivalent analysis," *IEEE Trans. Energy Convers.*, vol. 25, no. 1, pp. 148–160, Mar. 2010.

[14] W. Yang, K. Lee, S. Junker, and H. Ghezel-Ayagh, "Fuzzy fault diagnosis and accommodation system for hybrid fuel-cell/gas-turbine power plant," *IEEE Trans. Energy Convers.*, vol. 25, no. 4, pp. 1187–1194, Dec. 2010.

[15] L. Xu, J. Li, M. Ouyang, J. Hua, and X. Li, "Active fault tolerance control system of fuel cell hybrid city bus," *Int. J. Hydrogen Energy*, vol. 35, no. 22, pp. 12510–12520, 2010.

[16] D. Feroldi, "Fault diagnosis and fault tolerant control of PEM fuel cell systems," in *PEM Fuel Cells With Bio-Ethanol Processor Systems*. New York, NY, USA: Springer, 2012, pp. 185–206.

[17] I. Markovsky, "Closed-loop data-driven simulation," *Int. J. Control*, vol. 83, no. 10, pp. 2134–2139, 2010.

[18] M. Safonov and T. Tsao, "The unfalsified control concept and learning," vol. 42, no. 6, pp. 843–847, 1997. Q8

[19] M. Stefanovic and M. Safonov, *Safe Adaptive Control*. New York, NY, USA: Springer, 2011.

[20] E. Nabati and S. Engell, "Data-driven adaptive control: Making unfalsified control work better," in *Proc. 18th World Congr. Int. Fed. Autom. Control*, Milano, Italy, 2011, pp. 1285–1290.

[21] A. Neamtu and A. Stoica, "Unfalsified Control: Application to automatic flight control system design," *NCAS Bull.*, vol. 3, no. 3, pp. 103–114, 2011.

[22] A. Wolniakowski and A. Mystkowski, "Application of unfalsified control theory in controlling MAV," *Solid-State Phenom.*, vol. 198, pp. 171–175, 2013.

[23] J. van Helvoort, B. de Jager, and M. Steinbuch, "Unfalsified control using an ellipsoidal unfalsified region applied to a motion system," in *Proc. 16th World Congr. Int. Fed. Autom. Control*, Prague, Czech Republic, 2005, pp. 1–6.

[24] J. van Helvoort, B. de Jager, and M. Steinbuch, "Direct data-driven recursive controller unfalsification with analytic update," *Automatica*, vol. 43, no. 12, pp. 2034–2046, 2007.

[25] C. Kunusch and F. Castaños, "Extremum seeking algorithms for minimal hydrogen consumption in pem fuel cells," in *Proc. Amer. Control Conf.*, Washington, DC, USA, 2013, pp. 1144–1149.

[26] C. Ocampo-Martinez, R. S. Sánchez-Peña, F. Bianchi, and A. Ingimundarson, "Integrating unfalsified control and fault diagnosis for fault-tolerant control," *Int. J. Syst. Sci.*, 2014, to be published. Q9

[27] J. Zhang, G. Liu, W. Yu, and M. Ouyang, "Adaptive control of the airflow of a PEM fuel cell system," *J. Power Sources*, vol. 179, no. 2, pp. 649–659, 2008.

Fernando D. Bianchi received the B.S. and Ph.D. degrees in electronic engineering from the National University of La Plata (UNLP), Buenos Aires, Argentina, in 1999 and 2005, respectively.

From 1999 to 2006, he was a Postdoctoral Fellow at the Laboratory of Industrial Electronic, Control, and Instrumentation, UNLP. From 2006 to 2010, he was a Postdoctoral Researcher at the Technical University of Catalonia, Barcelona, Spain. In 2010, he joined the Power Electronics and Electric Power Grids Group, Catalonia Institute for Energy Research, Barcelona, as a Scientific Researcher. His main research interests include robust control and linear parameter-varying systems and their applications to the control of renewable energy conversion systems.

Carlos Ocampo-Martinez (S'97–M'12–SM'13) received the Electronic Engineering degree and the M.Sc. degree in industrial automation from the National University of Colombia, Manizales, Colombia, in 2001 and 2003, respectively, and the Ph.D. degree in control engineering from the Technical University of Catalonia, Barcelona, Spain, in 2007.

In 2008, as a Postdoctoral Fellow of the ARC Centre of Complex Dynamic Systems and Control, University of Newcastle, Australia, he was with the Spanish National Research Council, Institut de Robòtica i Informàtica Industrial, Barcelona, as a *Juan de la Cierva* Research Fellow. Since 2011, he has been an Assistant Professor at the Automatic Control Department, Technical University of Catalunya, Barcelona. His main research interests include the areas of constrained model predictive control, large-scale systems management, and nonlinear dynamics and industrial applications. Q10

Cristian Kunusch (S'03–M'10) received the B.S., M.Sc., and Ph.D. degrees in electronic engineering from the National University of La Plata, Buenos Aires, Argentina, in 2003, 2006, and 2009, respectively.

In 2010, he was appointed as a Postdoctoral Fellow of the Spanish National Research Council, Institut de Robòtica i Informàtica Industrial, Barcelona, Spain. In 2014, he joined the Electric Drives Predevelopment Team of Brose Fahrzeugteile, Würzburg, Germany, as a Senior Researcher. His main research interests include variable structure systems and their applications to the control and observation of fuel-cell-based systems and electric drives.

Ricardo S. Sánchez-Peña (S'86–M'88–SM'00) received the Electronic Engineer degree from the University of Buenos Aires (UBA), Buenos Aires, Argentina, in 1978, and the M.Sc. and Ph.D. degrees in electrical engineering from the California Institute of Technology, Pasadena, CA, USA, in 1986 and 1988, respectively.

In Argentina, he was with CITEFA, CNEA, and the space agencies CNIE Q11 and CONAE. He collaborated with NASA in aeronautical and satellite projects, and with the German (DLR) and Brazilian (CTA/INPE) space agencies. He was Q12 a Full Professor at UBA from 1989 to 2004, an ICREA Senior Researcher at the Universitat Politcnica de Catalunya, Barcelona, Spain, from 2005 to 2009, and a Visiting Professor/Researcher at several universities in the USA and the EU. He has consulted for ZonaTech (USA), STI, and VENG (Argentina) in aerospace Q13 applications, and with Alstom-Ecotecnia (Spain) in wind turbine applications. Since 2009, he has been a Director of the Ph.D. Department in Engineering, Buenos Aires Institute of Technology, Buenos Aires, and is a CONICET Q14 Principal Investigator. He has applied identification and control techniques to acoustical, mechanical, and aero and astronautical engineering, and also to type I Diabetes.

Dr. Sánchez-Peña received the Premio Consagración in Engineering by the National Academy of Exact, Physical, and Natural Sciences, Argentina, and the Group Achievement Award from NASA as a Review Board Member for the Aquarius/SAC-D satellite.

QUERIES

Q1. Author: Acronym “PEMFC” is used for two different terms in the paper. Please check.
Q2. Author: Please provide expanded form of CICYT, CONICET, PRH.
Q3. Author: Please provide expanded form of MACPERCON, CSIC.
Q4. Author: Please provide expanded form of CONICET and location details including postal code
Q5. Author: Please provide expanded form of LQR/LQG.
Q6. Author: Please provide legends for subparts in figures 5-10.
Q7. Author: Please provide journal name for reference 3.
Q8. Author: Please provide journal name for reference 18.
Q9. Author: Please update Ref. [26].
Q10. Author: Please ptovide expanded form of ARC, and location details of University of Newcastle, Australia.
Q11. Author: Please ptovide expanded form of CITEFA, CNEA, CNIE, CONAE and also provide location details.
Q12. Author: Please ptovide expanded form of DLR, CTA/INPE, ICREA.
Q13. Author: Please provide query for full location details of ZonaTech (USA), DLR, CTA/INPE, STI, VENG (Argentina), and Alstom-Ecotecnia (Spain).
Q14. Author: Please provide expanded form of CONICET and SAC-D.

Fault-Tolerant Unfalsified Control for PEM Fuel Cell Systems

Fernando D. Bianchi, Carlos Ocampo-Martinez, *Senior Member, IEEE*, Cristian Kunusch, *Member, IEEE*, and Ricardo S. Sánchez-Peña, *Senior Member, IEEE*

***Abstract*—This paper addresses the implementation of a data-driven control strategy in a real test bench based on proton exchange membrane fuel cells (PEMFCs). The proposed control scheme is based on unfalsified control, which allows adapting in real time the control law by evaluating the performance specifications based only on measured input–output data. This approach is especially suitable to deal with nonlinearity, model uncertainty, and also possible faults that may occur in PEMFCs. The control strategy has been applied to several experimental practical situations in order to evaluate not only the system performance, but also different fault scenarios. The experimental results have shown the effectiveness of the proposed approach to regulate the oxygen stoichiometry in real-time operation, as well as to maintain a proper system performance under fault situations. Also, a start-up mass-flow controller is added in order to bring the system toward its normal operating conditions.**

Q1

***Index Terms*—Fault-tolerant control (FTC) tests, oxygen stoichiometry, polymer electrolyte membrane fuel cells (PEMFCs), unfalsified control (UC).**

I. Introduction

THE EVOLUTION of modern society has been mostly based on the consumption of fossil fuel for electricity Q2 generation and the functioning of critical infrastructures such as transport networks. This model is strongly dependent on the constantly decreasing reserves of that type of fuel, which is also related to hazardous problems such as global warming. However, there are several options for electricity generation beyond fossil fuels that could mitigate the dependence modern society has with these scarce and polluting resources. Clean energy sources and, in particular, fuel cells (FCs) as electrochemical devices that generate electrical energy from hydrogen and oxygen, with pure water and heat as byproducts, are regarded as one of the most promising technologies due to their potential efficiency, compactness, and reliability [1]. Important advances in the design of these devices as well as on their materials allow to consider FCs viable for electricity generation not only at small scale (automotive), but also as technologies embedded in complex arrays of polygeneration such as the so-called smart energy grids [2]. In particular, polymer electrolyte membrane FCs (PEMFCs) are a type of FCs especially developed for both portable and stationary applications. Their distinguished features include lower pressure ranges, temperatures from 45 to $95\,^{\circ}\mathrm{C}$ and a special polymer electrolyte membrane (conducting hydrogen protons) [3].

Despite the notorious advantages of these devices and the widespread availability of hydrogen as a fuel, several technological challenges related to the PEMFC efficiency, lifetime, and economical costs are still open as major limitations for their standard implementation in everyday solutions. This fact, together with the recent advances in material sciences and component enhancements, makes advanced control techniques appear as complementary strategies in order to reduce costs, improve performance, and optimize efficiency, therefore increasing the lifetime of PEMFC-based systems. Hence, reliable control systems may ensure system stability and performance, as well as robustness against uncertainties and exogenous perturbations, all properties of capital importance for PEMFC success. Several research works have addressed the oxygen stoichiometry control to optimize the system conversion efficiency, avoiding performance deterioration together with eventual irreversible damages in the polymeric membranes due to oxygen starvation. These works present the way to achieve the aforementioned control objective by using different techniques: model predictive control (MPC) [4], sliding-mode control [5], full-state feedback with integral control [6] or LQR/LQG-based control [7], linear Q5 parameter varying control [8], and adaptive control [9], among others.

One important aspect when controlling real systems is concerned with the occurrence of component faults and their influence in the overall system performance. In fact, faults and model/sensor/actuator uncertainty play similar roles, then the conceptual distinction among them represents the difference between *active*[1] and *passive*[2] fault-tolerant control (FTC)

[1]Active FTC strategies aim at adapting the control loop based on the information provided by an FDI module within the fault-tolerant architecture.

[2]In passive FTC strategies, a single-control law is used in both faultless and faulty operation, assuming a certain degree of performance degradation.

Manuscript received February 15, 2014; revised July 7, 2014; accepted August 13, 2014. The work of C. Ocampo-Martinez and C. Kunusch was supported by the Project MACPERCON (Ref. 201250E027) of the CSIC. The work of Q3 C. Kunusch was supported by the seventh Framework Programme of the European Union through the Marie Curie actions (GA: PCIG09-GA-2011-293876) and the Puma-Mind Project (GA: FCH-JU-2011-1-303419), as well as by the CICYT Project DPI2011-25649 (MICINN-Spain). The work of R. S. Sánchez Q4 Peña was supported by CONICET and Grant PICT2008-290 from the PRH Program of the Ministry of Science, Technology, and Innovation of Argentina. Paper no. TEC-00097-2014.

F. D. Bianchi is with the Department of Electrical Engineering, Catalonia Institute for Energy Research, 08930 Barcelona, Spain (e-mail: fbianchi@irec.cat).

C. Ocampo-Martinez and C. Kunusch are with Institut de Robtica i Informtica Industrial, Universitat Politècnica de Catalunya, 08028 Barcelona, Spain (e-mail: cocampo@iri.upc.edu; ckunusch@iri.upc.edu).

R. S. Sánchez-Peña is with CONICET and the Instituto Tecnológico de Buenos Aires, C1106ACD Buenos Aires, Argentina (e-mail: rsanchez@itba.edu.ar).

Color versions of one or more of the figures in this paper are available online at http://ieeexplore.ieee.org.

Digital Object Identifier 10.1109/TEC.2014.2351838

design approaches [10]. In the framework of FCs and assuming an active FTC architecture, several approaches for fault detection and isolation (FDI) have been proposed. Model-based FDI for PEMFC systems based on consistency relations for the detection and isolation of predefined faults has been proposed in [11], while in [12], a comparison of both model-based and data-driven fault detection methods for FCs is addressed. The work in [13] proposes a methodology to use the electrical model for FC system diagnosis, while in [14], a fault diagnosis and accommodation system based on fuzzy logic has been developed as an effective complement for a closed-loop scheme. Regarding FTC, Xu *et al.* [15] present an experimental implementation of an active FTC system for an FC/battery hybrid power train applied to a city bus, while Feroldi [16] proposes an MPC scheme for adding fault tolerance capabilities to a two-actuator PEMFC system.

Unfalsified control (UC) theory was born as an approach for data-driven control, where no prior hypothesis on the plant is used besides the measured data streams [17]. The control law is selected from a predefined set by the performance evaluation based solely on the information provided by the measured input–output (I/O) data. The controllers that do not achieve the desired performance specifications are discarded (falsified). Instead, one of the remaining (unfalsified) controllers is used, until it is falsified by the past measurements and replaced by a new UC and so on. This technique has been formally introduced by Safonov and Tsao [18]. UC is a real-time implementation method that may be combined with other model-based design techniques, hence it is not mutually exclusive [19].

At this point, UC emerges as an especially suitable technique to tackle the complex characteristics inherent to FC systems. Nonlinear dynamics, inaccessible variables, and model uncertainties are natural addresses by UC. Being a data-driven approach, UC is also particularly suited for dealing with unknown disturbances and possible fault occurrences. The application of UC in other systems has been previously reported in the literature and ranges from chemical reactors [20], flight control systems [21], up to microaerial vehicles [22], among others. In [23], the implementation of an ellipsoidal UC (EUC) in a dual rotary fourth-order motion system is presented, showing the success of the experimentation by ensuring the convergence of the proposed algorithm. By a suitable selection of the controller set and the performance test, EUC is capable of an efficient implementation of UC ideas as a convex optimization problem easily implemented in real time. From the best of the author's knowledge, UC has never been implemented in the control/supervision of a complex system based on PEMFCs.

The main contribution of this paper is a robust oxygen stoichiometry control design based on UC and its implementation in a laboratory FC system. In particular, an EUC-based closed-loop scheme [24] is designed and tested experimentally under several scenarios. The control objectives cover the traditional stoichiometry regulation, disturbance rejection represented by changes in the load profile of the PEMFC, and also the consideration of actual fault events in the components, which may induce performance loss and hazardous operation of the entire system. The proposed approach may be integrated into a multilevel supervisory control scheme, where other system variables might be simultaneously regulated toward the improvement of global objectives such as durability and efficiency of the overall PEMFC system [25]. Experimental results have shown the effectiveness of the proposed approach in fulfilling the control objective (stoichiometry regulation) in real-time system operation. The overall scheme proposed in this paper also includes a start-up mass-flow control strategy, which avoids an abrupt/nonsmooth behavior of the system variables when the EUC controller is started with initial conditions far away from the nominal system operation. The scheme proposed in this paper introduces fault tolerance capabilities as in [26], but considering the proposed fault scenarios over the real experiment.

The remainder of this paper is organized as follows. Section II briefly describes the physical system and control objectives as well as the main parts of the experimental test bench. Section III introduces the EUC techniques as well as the necessary modifications in order to implement it in the real case presented here. Section IV collects and explains in detail the experimental results for different practical scenarios, and Section V presents the main conclusions.

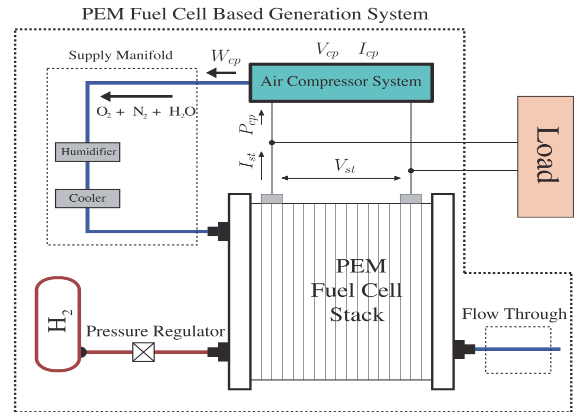

Fig. 1. Schematic diagram of the PEMFC-based generation system.

II. System Physical Description

The system is comprised by a central PEMFC stack and additional/complementary units. In Fig. 1, the scheme of the considered system and the interaction between its different subsystems (FC stack, reactant supply system, and humidity management unit) is shown. A brief description of some components, variables, and processes is presented as follows. In the system, the control input u corresponds to the compressor voltage denoted V_{cp}. The system output y corresponds in turn to the inlet stoichiometry of the PEMFC cathode, namely λ_{O_2}. Moreover, the system is affected by the external disturbance I_{st}, which corresponds to the stack current flowing toward the load.

The main subsystems depicted in Fig. 1 are as follows:

1) a 12-V dc air compressor with an oil-free diaphragm vacuum pump, whose input voltage V_{cp} is the control variable (as established beforehand);
2) hydrogen and oxygen cellkraft membrane exchange humidifiers and line heaters, which are used to maintain

proper humidity and temperature conditions inside the cell stack[3];

3) a ZBT 8 fuell-cell stack with Nafion 115 membrane electrode assemblies with 50 cm^2 of active area and 150-W power.

Moreover, different sensors are incorporated into the system such as an air-mass flowmeter (range 0–15 slpm) at the end of the compressor to measure its flow ($W_{\rm cp}$), a current clamp (range 0–3 A) and a voltage meter (range 0–15 V) to measure the motor stator current ($I_{\rm cp}$) and voltage ($V_{\rm cp}$), respectively. Besides, temperature sensors are arranged in order to register the different operation conditions. The full description of this system, as well as a fully validated nonlinear dynamic model specially developed for control purposes are presented and deeply discussed in [3]. Given the complexity of the nonlinear model and the consequent difficulty for designing and implementing online controllers, data-driven control techniques rise as an attractive alternative for real-time operation of such systems, mainly when different experimental scenarios are considered.

In order to maximize the efficiency of the PEMFC system, the regulation of the oxygen mass inflow toward the stack cathode should be achieved. Additionally, oxygen starvation and irreversible membrane damage are averted. To accomplish such an oxidant flow is equivalent to maintaining the oxygen excess ratio of the cathode at a suitable value. The oxygen excess ratio or oxygen stoichiometry is defined as

$$\lambda_{O_2} = \frac{W_{O_2,\rm ca}}{W_{O_2,\rm react}} \tag{1}$$

where $W_{O_2,\rm react}$ is the oxygen flow consumed in the reaction and $W_{O_2,\rm ca}$ is the oxygen partial flow entering the cathode, which depends on the air flow released by the compressor $W_{\rm cp}$, i.e.,

$$W_{O_2,\rm ca} = \frac{\chi_{O_2} W_{\rm cp}}{1+\omega_{\rm amb}}. \tag{2}$$

Here, $\omega_{\rm amb}$ is the ambient air humidity ratio and χ_{O_2} is the molar fraction of oxygen in the air ($\chi_{O_2} = 0.21$). As $W_{O_2,\rm ca}$ is an internal unavailable variable of the system, it is not practical to include it in the control algorithm. This problem was circumvented by inferring information of $W_{O_2,\rm ca}$ from an accessible variable of the system, such as the air-mass flow delivered by the compressor

$$\begin{aligned} W_{\rm cp} = \; & B_{00} + B_{01}\omega_{\rm cp} + B_{02}\omega_{\rm cp}^2 \\ & + (B_{10} + B_{01}\omega_{\rm cp})\Psi + B_{02}\Psi^2 \end{aligned}$$

being $\Psi = m_{a,\rm hum} T_{\rm hum} R_a / V_{\rm hum} + K_{\rm hum}$, $\omega_{\rm cp}$ is the compressor speed, and $m_{a,\rm hum}$ is the humidifier mass of air. The compressor parameters B_{00}, B_{01}, B_{10}, B_{11}, B_{02}, and B_{20} can be obtained from [5], $T_{\rm hum}$ is the humidifier temperature, $V_{\rm hum}$ is the humidifier volume, R_a is the air gas constant, and $K_{\rm hum} = P_{\rm sat}(T_{\rm hum}) RH_{\rm hum} - P_{\rm sat}(T_{\rm amb}) RH_{\rm amb}$, with $P_{\rm sat}(T_{\rm hum})$ being the vapur saturation pressure at $T_{\rm hum}$, $RH_{\rm hum}$ the relative humidity of the gas at the humidifier output, $P_{\rm sat}(T_{\rm amb})$ the vapur saturation pressure at ambient temperature, and $RH_{\rm hum}$ the relative humidity of ambient air.

Note that $W_{O_2,\rm react}$ is directly related to the stack current as follows:

$$W_{O_2,\rm react} = G_{O_2} n I_{st} / 4F \tag{3}$$

with G_{O_2} is the molar mass of oxygen, n is the number of cells, and F is the Faraday's constant. As presented in the validated model [3], the operating conditions of the system inputs are determined by $V_{\rm cp}$ and $I_{\rm st}$.

This paper is focused on the oxygen stoichiometry λ_{O_2} tracking under continuous changes in the load condition $I_{\rm st}$, such that

$$e_\lambda = \lambda_{O_2} - \lambda_{O_2,\rm ref} \tag{4}$$

is as small as possible for both nominal and fault conditions. In (4), $\lambda_{O_2,\rm ref}$ corresponds to a given reference value, which comes from a supervisory controller that considers global objectives related to the efficiency and durability of the overall PEMFC-based system [25].

III. UC of PEMFCs

The UC concept proposed by [18] consists of a set of candidate controllers $\mathbf{K}$ and a switching algorithm that selects the most suitable controller in the set according to a performance criterion based only on experimental I/O data. The main appeal of UC is that there is no need of a plant model to decide if a controller satisfies the performance specifications.

The only *a priori* information needed about the system is a set of I/O measures $\mathcal{Z}(k) = \{(u(l), y(l)), 0 \le l \le k\}$, with k being the discrete time. The performance specifications are stated as a cost-function $\mathcal{V}$ depending on the reference r, and on the input u and output y. As a consequence, the performance specifications define a subset

$$\mathcal{T}_{\rm spec} = \{(r, u, y) : \mathcal{V}(r, u, y) < \eta\}$$

where η is a positive scalar bounding the performance specifications. In turn, a candidate controller $K \in \mathbf{K}$ also defines a subset

$$\mathcal{K} = \{(r, u, y) \; : \; u = K(r, y)\}$$

where K must be "causally-left-invertible," i.e., there exists K^{-1} that allows the computation of a fictitious reference r_f from (u, y). This reference is the value that r would take if the controller K is inserted in the loop, and the I/O of the plant were (u, y). The fictitious reference can be computed from $\mathcal{Z}$ and K, without actually inserting the controller in the loop, as follows:

$$r_f = K^{-1}(u, y). \tag{5}$$

In this framework, the controller K is said to be unfalsified by the experimental information $\mathcal{Z}$ if

$$\mathcal{K} \cap \mathcal{Z} \cap \mathcal{T}_{\rm spec} \neq \emptyset \tag{6}$$

otherwise the controller is said to be falsified by the measured data. The problem is feasible if the set of candidate controllers

[3]Decentralized PID controllers are in charge of ensuring the adequate operation values for these devices; therefore, this control design is out of the scope of this paper.

includes at least one which stabilizes the system (see [19, p. 18]).

The selection of the most adequate controller, also denoted the falsification procedure, according to the *a posteriori* information (u, y) relies on the evaluation of a cost-detectable function. This property guarantees stability and convergence of the adaptive procedure.

The controller set may have a finite or infinite number of controllers. In the first case, all the controllers in the set are tested simultaneously. That could be computationally demanding if it contains a large number of controllers. In the second approach, the set is defined by a control structure that updates its parameters in real time. The selection of the most suitable controller relies on an optimization procedure that computes the best controller parameters. This option could be more computationally efficient but is limited to certain cost functions. Hence, the proper selection of these cost functions is done in such a way that the controller selection results in a convex optimization easy to solve online. The UC technique used here is based on this latter approach.

A. Ellipsoid Unfalsified Control

The cost function and the controller structure define the falsifier complexity. In particular, the EUC, by selecting an adequate cost function and a certain control structure, computes the most suitable controller by means of an efficient convex optimization procedure and with proven convergence properties [24]. Most precisely, the controllers are parameterized as

$$u(k) = \begin{bmatrix} r(k) \\ \Lambda_u(z^{-1})u(k) \\ y(k) \\ \Lambda_y(z^{-1})y(k) \end{bmatrix}^T \begin{bmatrix} 1/\hat{\theta}_1 \\ -\hat{\theta}_2/\hat{\theta}_1 \\ -\hat{\theta}_3/\hat{\theta}_1 \\ -\hat{\theta}_4/\hat{\theta}_1 \end{bmatrix} \quad (7)$$

where Λ_u and Λ_y are stable linear filters, $\hat{\theta}_i$ $(i = 1, \ldots, 4)$ are parameters to be set online, and z is the unity delay. With this parameterization, the fictitious reference can be found as

$$r_f(k) = w^T(u, y, k)\theta \quad (8)$$

where

$$w = \begin{bmatrix} u(k) \\ \Lambda_u(z^{-1})u(k) \\ y(k) \\ \Lambda_y(z^{-1})y(k) \end{bmatrix}, \quad \theta = \begin{bmatrix} \theta_1 \\ \theta_2 \\ \theta_3 \\ \theta_4 \end{bmatrix}.$$

The controller parameterization and the computation of the fictitious references are illustrated in Fig. 2. Note the difference between the parameter $\hat{\theta}$ of the current controller and the parameter θ under performance evaluation by the UC algorithm.

The performance criterion is cast in the form of model reference tracking as

$$|e_f(\theta, k)| + \kappa|u(k)| \leq \Delta(k) \quad (9)$$

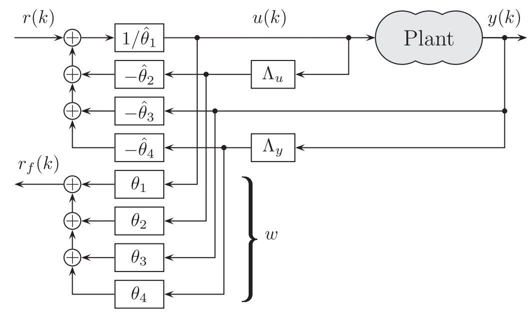

Fig. 2. Controller parameterization and fictitious reference computation.

where $e_f(k) = G_m(z^{-1})r_f(\theta, k) - y(k)$, G_m is a stable system that defines the desired behavior, and $\Delta(\cdot)$ is a time-dependent bound. Then, the set of controller parameters that satisfy the performance specifications is given by

$$\mathcal{U}(k) = \{\theta \, : \, -\hat{\Delta}(k) \leq e_f(\theta, k) \leq \hat{\Delta}(k)\} \quad (10)$$

where $\hat{\Delta}(k) = \Delta(k) - \kappa|u(k)|$. The set of controllers is given by (7) and the parameter set

$$\mathcal{E}(k) = \{\theta \, : \, (\theta(k) - \theta_c(k))^T \Sigma(k)(\theta(k) - \theta_c(k))\} \quad (11)$$

where $\mathcal{E}(k)$ is an ellipsoid of center $\theta_c(k)$ and size is defined by the positive-definite matrix $\Sigma(k)$ [24].

With these definitions, the controller and specification sets are parameterized in θ and condition (6) results in

$$\mathcal{E}(k) \bigcap \mathcal{U}(k) \neq \emptyset. \quad (12)$$

That is, the set of UCs is given by the parameters θ in the intersection of $\mathcal{E}(k)$ and $\mathcal{U}(k)$. Therefore, the falsification algorithm reduces to shrinking the ellipsoid volume ($\mathrm{vol}(\mathcal{E}(k))$) by changing the matrix $\Sigma(k)$, to check the intersection of $\mathcal{E}(k)$ and $\mathcal{U}(k)$, and to select a new $\hat{\theta} \in \{\mathcal{E}(k) \bigcap \mathcal{U}(k)\}$.

The original EUC algorithm was intended for time-invariant systems and the volume of the ellipsoid was reduced as long as the *a posteriori* information increased, and thus, the controller parameters converged to the controller that satisfied the performance specifications. In other words, when the number of samples of (u, y) increases, the information is used to remove those controllers that do not satisfy the performance criterion. In case of time-varying or nonlinear systems, a controller falsified for certain operating conditions could satisfy the performance criterion in other operating points. Therefore, the EUC algorithm needs some modification in order to cover these cases. Here, the expansion of the ellipsoidal volume, when no controller is falsified, is proposed. More precisely, if the current controller parameter are not falsified after k_{th} samples, the ellipsoid volume $\mathrm{vol}(\mathcal{E}(k))$ is expanded by changing the matrix Σ as follows:

$$\Sigma(k+1) = \Sigma(k)\beta^p$$

where $\beta > 1$ and p increases by 1, each time the current controller remains unfalsified during more than k_{th} samples. The expansion continues until the controller is falsified or the initial volume is reached.

B. EUC for PEMFC

To design an EUC control algorithm it is necessary to choose the filters Λ_u and Λ_y, which define the controller set and the transfer function G_m to define the desired behavior. Although EUC does not require *a priori* information of the plant, it is always useful to have a rough idea about its dynamics and the structure needed to achieve the desired closed-loop behavior.

In the case of the PEMFC, the system behavior around an operating point can be roughly approximated by a second-order system of the form

$$G(z) = \frac{\lambda_{O_2}(z)}{V_{\mathrm{cp}}(z)} = K_{fc}\frac{z-a}{(z-b)(z-c)}. \tag{13}$$

By selecting

$$\Lambda_u(z) = \Lambda_y(z) = \frac{K_\Lambda}{z-q} \tag{14}$$

and the control law

$$u(k) = \frac{1}{\theta_1}r(k) - \frac{\theta_2}{\theta_1}\cdot\frac{K_\Lambda}{z-q}u(k) - \left(\frac{\theta_3}{\theta_1} + \frac{\theta_4}{\theta_1}\cdot\frac{K_\Lambda}{z-q}\right)y(k) \tag{15}$$

and for the particular values $\theta_3 = 1$ and $\theta_4 = 0$, the controller results

$$u(k) = \frac{1}{\theta_1}\cdot\frac{z-q}{z-(q-\theta_2 K_\Lambda/\theta_1)}(r(k)-y(k)). \tag{16}$$

With proper values of θ_1 and θ_2, it is possible to obtain a closed-loop transfer function of the form

$$G_{cl}(z) = \frac{\lambda_{O_2}(z)}{\lambda_{O_2,\mathrm{ref}}(z)} = \frac{K_{cl}}{z-q_{cl}}. \tag{17}$$

Therefore, it is reasonable that the desired closed-loop behavior given by G_m has the form of G_{cl} in (17).

IV. Experimental Results

This section describes the different scenarios considered for testing the effectiveness of the proposed control approach. For every scenario, the main results are discussed through the most relevant variables involved in each case. They include typical performance tests and the effect of faults in different parts of the PEMFC-based system. Before analyzing the experimental results, a brief description of the experimental test bench and the particular EUC settings are presented.

A. Workplace Setup

The control strategy was implemented in a complete data acquisition and control system. It is composed of two computers (each with four i5 core processors at 2.6-GHz clock frequency): the host and the real-time operating system. The former provides the software development environment and the graphical user interface. It is responsible for the startup, shutdown, configuration changes, and control settings during operation. The latter implements the control algorithms and the data acquisition via a field-programmable gate array in order to have high-speed data processing. Control, security, and monitoring tasks are conducted by a CompactRIO (reconfigurable I/O) system from National Instruments. In order to record the analog sensor signals, a 32-channel 16-bit analog input module from National Instruments is used (NI-9205). An eight-channel, digital I/O module generates the necessary transistor–transistor logic signals for different security and diagnostic tools. Fig. 3 shows the laboratory setup used in the experiments.

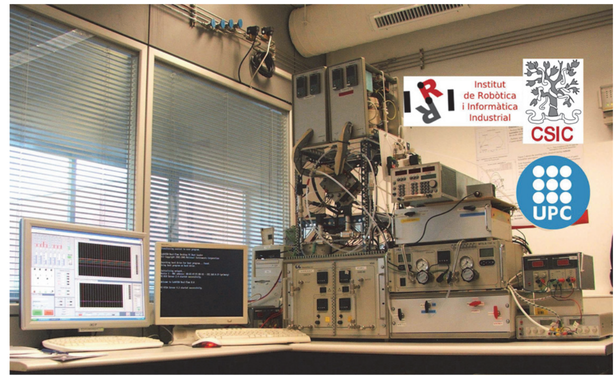

Fig. 3. Picture of the laboratory test station at IRI (CSIC-UPC).

B. EUC Controller Setup

The EUC algorithm has been developed in MATLAB and then crosscompiled into a LabView environment by means of a *DLL* file obtained through the MATLAB real-time workshop toolbox.

The tracking error was bounded with the function

$$\Delta(k) = 0.25 + 1.9\mathrm{e}^{-0.02k}$$

which ensures a 2% tracking error and relaxes the error during the initial transients, avoiding excessive controller falsifications.

The filters were selected as

$$\Delta_y(z) = \Delta_u(z) = \frac{0.00897}{z-0.991}$$

and the reference model as

$$G_m(z) = \frac{0.0198}{z-0.9802}.$$

These transfer functions were selected based on linear models identified at several operating points; therefore, the adopted control structure allows achieving the desired closed-loop behavior. The sampling time was 0.01 s.

The initial value of the controller parameters was

$$\theta_0 = \begin{bmatrix} 2 & -1.99 & 1 & 0 \end{bmatrix}^T.$$

The parameters for the expansion of the ellipsoid volume were set as $\beta = 1.5$ and $k_{\mathrm{th}} = 100$.

C. Complete Control Strategy

The UC is complemented with a bumpless and a flow control to help in the startup of the system. This complementary start-up controller acts as a safety strategy to avoid undesired consequences in the FC stack durability, regulating the air-mass inflow from the compressor. Thus, W_{cp} is regulated toward a convenient value in such a way that λ_{O_2} reaches values close

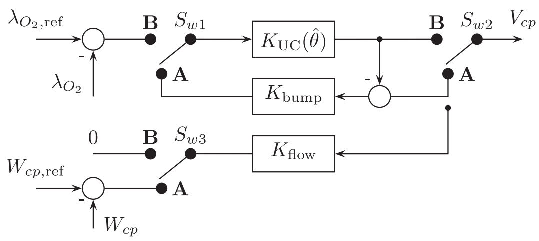

Fig. 4. Complete control scheme including the UC and the start-up controllers.

to its desired reference $\lambda_{O_2,\mathrm{ref}}$ [given that both variables W_{cp} and λ_{O_2} are related by means of (1) and (2)]. Therefore, a smooth starting behavior of λ_{O_2} is achieved. The complete control scheme is sketched in Fig. 4.

In this initial stage, the switches $S_{w1} = S_{w2} = S_{w3}$ are set at position **A** and the controller

$$K_{\mathrm{flow}}(z) = 0.43 + \frac{0.043}{z-1}$$

tracks a predefined profile leading the system to a suitable flow condition before starting the stoichiometry control. This PI controller was designed experimentally based on the step response of the system under the initial operating conditions to ensure a settling time lower than 1 s.

The bumpless controller

$$K_{\mathrm{bump}}(z) = 0.3175 + \frac{0.2}{z-1}$$

ensures a smooth transition from flow to stoichiometry control. This PI controller was designed to ensure that $K_{\mathrm{UC}}(\theta_0)$ achieves a rapid tracking of the signal V_{cp} produced by K_{flow}.

Once a preset time is reached, the $S_{w1} = S_{w2} = S_{w3}$ are set at position **B** and the control switches to stoichiometry control. Initially, the EUC starts with a fixed initial control given by θ_0. This can be a conservative controller that covers the complete operating envelope in a stable way, but with poor performance. Once the EUC is fully operative, the switching algorithm is responsible for finding a more suitable parameter θ to achieve a better performance in the actual operating conditions.

D. Experimental Scenarios

In order to evaluate the performance of the proposed closed-loop control scheme, the following realistic scenarios are considered for covering not only nominal (faultless) situations, but also the effect of real faults in the system. Note that these tests include a real set of safety measures and devices that avoid any hazardous behavior of the test bench (like over pressures, temperatures, or currents). The anode line is also monitored by a higher level supervisor, avoiding any irreversible damages in the cells due to high-differential pressure between anode and cathode.

1) Scenario 1 (Start-up Controller and Reference Tracking): This scenario considers two parts; the system behaviour with a start-up flow controller and the reference tracking performance. First of all, in order to carry the system variables toward an initial operation regime, the overall control structure considers the initial regulation of the compressor flow W_{cp} at a given value,

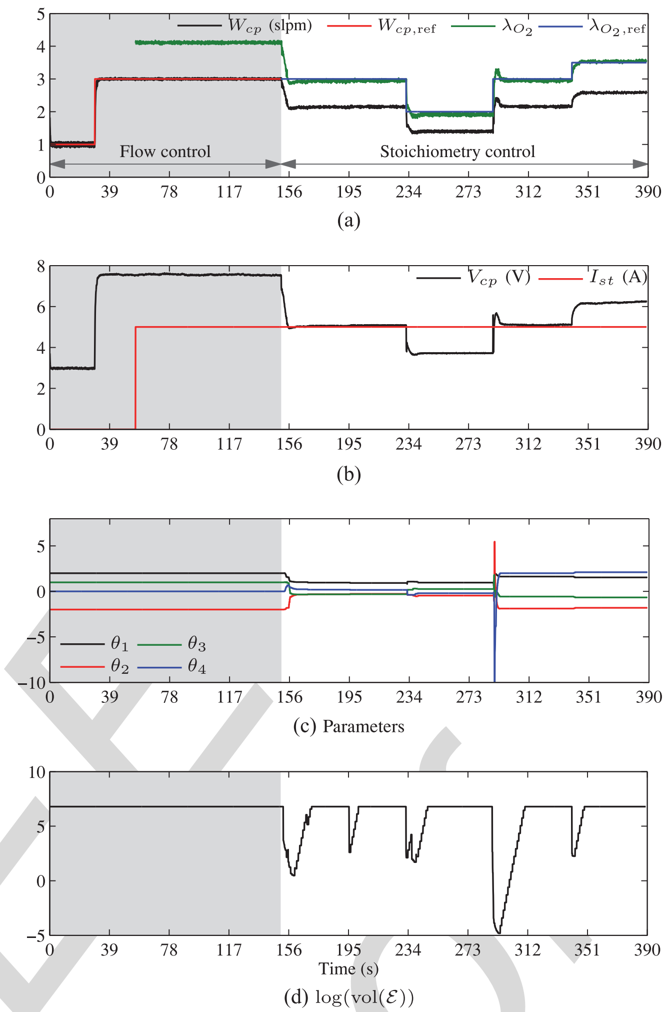

Fig. 5. Start-up and closed-loop response for several step changes in the stoichiometry reference (Scenario 1).

close enough to nominal operating points when the stack is delivering electrical power. In this initial stage, the falsification algorithm is out of the loop and will only be activated after W_{cp} reaches its reference value

$$W_{\mathrm{cp,\,ref}} = (1+\omega_{\mathrm{atm}})\lambda_{o2,\,\mathrm{ref}} G_{O_2} n I_{\mathrm{st}}/(4F\chi_{o2}).$$

Fig. 5 presents the behaviour of the system variables for this scenario. Note that the stoichiometry is not well defined, until I_{st} is greater than zero. Q6

After 150 s of flow regulation, the closed-loop system switches to an initial stabilizing controller ($\theta = \theta_0$) before activating the EUC controller at time $t = 152$ s [see the transitions in the ellipsoid volume parameter $\mathrm{vol}(\mathcal{E}(k))$ in Fig. 5(d)] and considers different values for the oxygen stoichiometry reference $\lambda_{O_2,\mathrm{ref}}$ ranging from 2 to 3.5. Here, the stack current I_{st} remains constant at 5 A. This is a typical scenario where the oxygen stoichiometry of a PEMFC-based system is changed to obtain different net powers. Although the flow control is no longer connected, W_{cp} follows the stoichiometry evolution due to their relation given by (1) and (2). Once the EUC is activated, notice the suitable change of parameters θ_i in Fig. 5(c), which

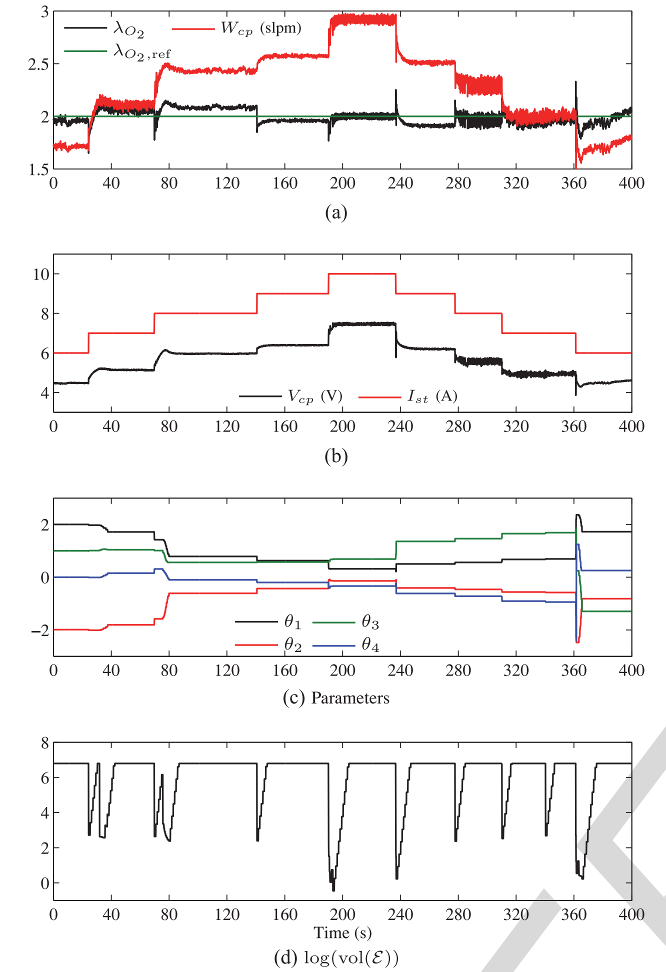

Fig. 6. Closed-loop response for several step changes in I_{st} (Scenario 2).

induces smooth changes in the control signal V_{cp} [see Fig. 5(b)] in order to adapt the controller to different operating conditions associated with the different values of $\lambda_{O_2,\mathrm{ref}}$. This reference can be directly computed offline or through an extremum seeking algorithm like the one presented in [25], where the goal is to optimize the overall system efficiency. The bottom plot shows the evolution of the ellipsoid volume $\mathrm{vol}(\mathcal{E}(k))$ (in logarithmic scale). It can be seen that after $k_{\mathrm{th}} = 100$ samples without any controller falsification, the algorithm expands the volume to be better prepared for new operating conditions.

2) Scenario 2 (Disturbance Rejection): Considering that the desired value of $\lambda_{O_2,\mathrm{ref}}$ is already reached, it is also important to evaluate the performance of the EUC-based closed-loop system when changes in the load current I_{st} take place. To reproduce this typical working case, $\lambda_{O_2,\mathrm{ref}}$ was set at 2, while different values of I_{st} have been required from the PEMFC stack. Fig. 6 shows the main variables related to this test. Note that λ_{O_2} is rapidly reaching the new steady state desired value after each change of I_{st}. Meanwhile, the parameters θ_i are being adapted to this end [see Fig. 6(c)], with changes in I_{st} between 6 and 10 A and smooth changes of the control signal V_{cp}. The lower plots shows the updates of the controller parameters and the changes in the ellipsoid volume $\mathrm{vol}(\mathcal{E}(k))$, when the operating

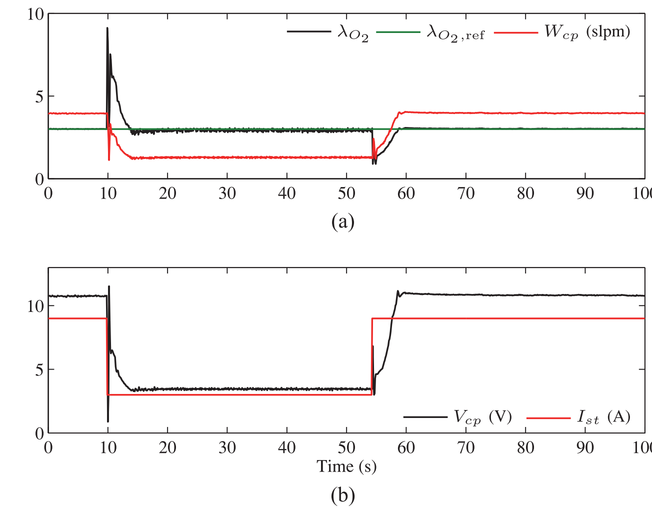

Fig. 7. Closed-loop response for 6 A step changes in I_{st} (Scenario 2).

conditions change as a consequence of changes in I_{st}. It can be seen that parameters θ_i change more than once for constant values of I_{st}. This is mainly a consequence of the noise in the measures of V_{cp}.

Besides, Fig. 7 shows the stoichiometry regulation under a demanding scenario, in which the current I_{st} increases and decreases in step changes of 6 A. Even under demanding conditions, the proposed EUC control scheme is capable of rapidly returning the stoichiometry to the set-point value. To properly handle these abrupt step changes, faster devices such as supercapacitors and/or batteries should be connected in parallel with the PEMFC system.

3) Scenario 3 (Cathode Outflow Fault): This scenario considers the effect of a couple of faults in the performance of the PEMFC-based system. Faults in this case are related to the cathode outflow in the following way 1) there is a flow blockage (FB) that causes the increase of the cathode inlet pressure P_{ca}, and 2) there is a flow leak (FL) that is compensated by increasing V_{cp} without affecting P_{ca}. The goal is to check the behavior of the EUC-based closed loop when rejecting these changes in the cathode line, while both I_{st} and λ_{O_2} remain constant at 5 A and 3, respectively, along the whole experiment. Fig. 8 shows the system variables related to this test. The magnitude of the FB fault can be quantified by either analyzing the behavior of P_{ca} [see Fig. 8(b)], or computing the compressor power by means of V_{cp} and I_{cp}, both plotted in the same figure. Since the FB fault appearing at $t = 35$ s progressively increases P_{ca}, the EUC controller suitably adapts the parameters during that effect (see transitions of $\mathrm{vol}(\mathcal{E}(k))$ after 35 s). In the case of the FL fault, its magnitude can be quantified by observing V_{cp}, since P_{ca} is not affected due to the compensation performed by the manipulated input after $t = 255$ s. It should be noticed that the proposed control scheme is capable to properly reject the effect of the considered faults, and after a slight deviation, λ_{O_2} returns to its desired reference value. The controller also allows to recover the system even when the fault disappears and the nominal behavior is recovered.

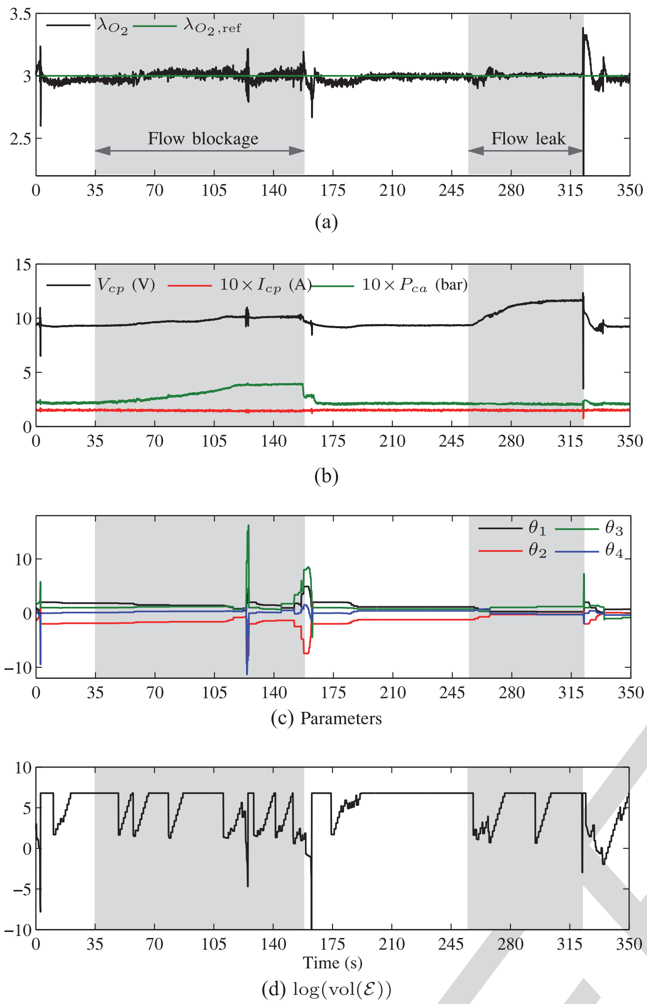

Fig. 8. Closed-loop response during FB and FL faults (Scenario 3).

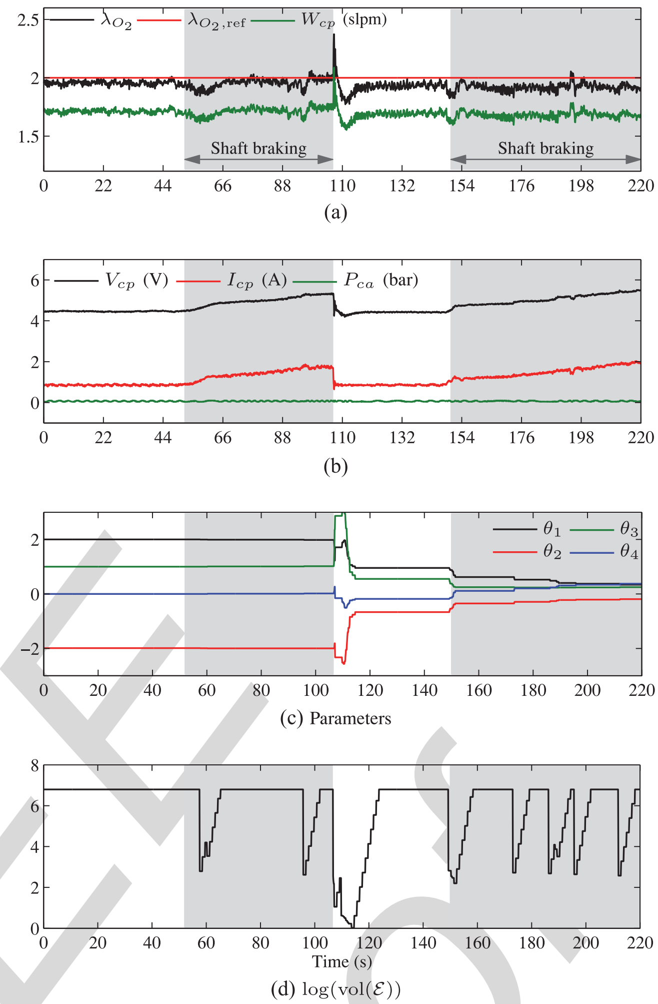

Fig. 10. Closed-loop response during a compressor fault (Scenario 4).

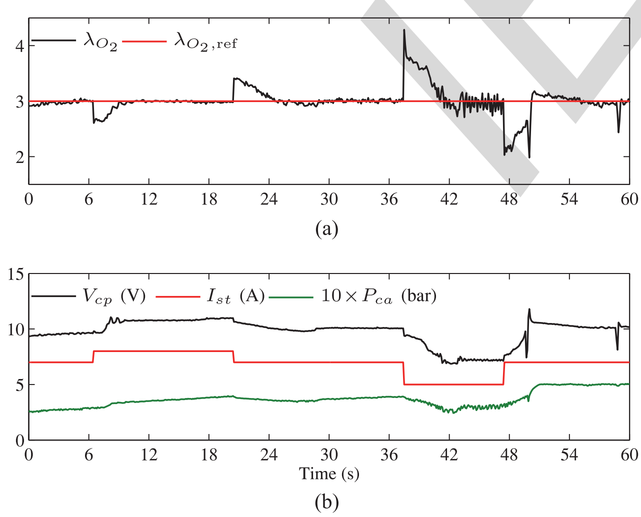

Fig. 9. Closed-loop response for I_{st} changes under an FB fault (Scenario 3).

As an additional evaluation of the proposed control scheme, Fig. 9 shows the disturbance rejection capability under a FB fault. The EUC controller reaches the proper recovery of λ_{O_2}, when several changes of I_{st} were performed.

4) Scenario 4 (Compressor Fault): Here, a different fault is considered, which is related to the capacity of the air supply from the compressor connected to the PEMFC cathode. The fault affects the compressor by changing the inertia and nominal friction of its motor shaft. Again, the goal is to check the behavior of the EUC-based closed loop when rejecting this fault, while both I_{st} and λ_{O_2} remain constant at 6 A and 2, respectively. Fig. 10 shows the system variables during this test. The magnitude of the fault in this case is strongly related to I_{cp}, but note that for this case, P_{ca} remains constant [see Fig. 10(b)]. The fault appears at time $t = 50$ s, disappears at $t = 106$ s, and appears again at $t = 146$ s. The EUC controller adapts the parameters θ_i conveniently, while reducing the stoichiometry regulation error as much as possible.

The results presented in this paper mainly highlight the implicit fault tolerance capabilities given by the EUC scheme (due to its data-driven control nature) independently of knowing the particular way the faults affect the system. As stated in the Introduction, several authors have reported the design and implementation of FTC techniques for PEMFC systems, which explicitly use the system model [15], [16] unlike the fault tolerance capabilities of the proposed model-free approach. On the other hand, reported adaptive schemes for PEMFCs address the manipulation of the air-mass flow for controlling λ_{O_2} [8], [27], and the online system identification and efficiency management by controlling λ_{O_2}, relative humidity, and stack temperature [9]. Although those approaches show experimental evidences of their proper operation under nominal conditions, they do not consider the effects of faults over the performance of the closed loop.

V. Conclusion

An FTC for PEMFC was proposed and experimentally tested in a laboratory test bench. The proposed control is based on EUC that allows adapting the controller parameters by evaluating the closed-loop performance solely from measures of the compressor voltage (control input) and the oxygen stoichiometry (controlled output). The EUC algorithm does not rely on a plant model, which makes it suitable for dealing with complex systems and also to tackle faults in the cathode outflow or in the compressor. Four experimental scenarios have shown that the proposed UC control is capable of effectively working in different operating conditions and most common faults in PEMFCs. A start-up mass-flow control strategy has also been introduced, which avoids abrupt changes in the system variables when the initial conditions are far away from the nominal values.

Acknowledgment

All the experimental tests were performed at the PEM Fuel Cells Laboratory, Institut de Robòtica i Informàtica Industrial (CSIC-UPC), Barcelona, Spain, and only possible due to its advanced equipment and proficient technical staff.

References

[1] U.S. Department of Energy, Hydrogen, Fuel Cells and Infrastructure Technologies Program: Multi-Year Research, Development And Demonstration Plan: Planned program activities for 2005–2015. DOE Website. Section 3.4 Fuel Cells, 2005.

[2] J. Blanchard, "Smart energy solutions using fuel cells," in *Proc. IEEE 33rd Int. Telecommun. Energy Conf.*, Amsterdam, The Netherlands, 2011, pp. 1–8.

[3] C. Kunusch, P. Puleston, M. Mayosky, and A. Husar, "Control oriented modelling and experimental validation of a PEMFC generation system," vol. 6, no. 3, pp. 851–861, 2011. Q7

[4] C. Ziogou, S. Papadopoulou, M. C. Georgiadis, and S. Voutetakis, "On-line nonlinear model predictive control of a PEM fuel cellsystem," *J. Process Control*, vol. 23, no. 4, pp. 483–492, 2013.

[5] C. Kunusch, P. Puleston, M. Mayosky, and L. Fridman, "Experimental results applying second order sliding mode control to a PEM fuel cell based system," *Control Eng. Pract.*, vol. 21, no. 5, pp. 719–726, 2013.

[6] J. Pukrushpan, A. Stefanopoulou, and H. Peng, *Control of Fuel Cell Power Systems*. New York, NY, USA: Springer, 2004.

[7] A. Niknezhadi, M. Allué-Fantova, C. Kunusch, and C. Ocampo-Martinez, "Design and implementation of LQR/LQG strategies for oxygen stoichiometry control in PEM fuel cells based systems," *J. Power Sources*, vol. 196, no. 9, pp. 4277–4282, 2011.

[8] F. Bianchi, C. Kunusch, C. Ocampo-Martinez, and R. S. Sánchez-Peña, "A gain-scheduled LPV control for oxygen stoichiometry regulation in PEM fuel cell systems," *IEEE Trans. Control Syst. Technol.*, vol. 22, no. 5, pp. 1837–1844, Sep. 2014.

[9] S. Kelouwani, K. Adegnon, K. Agbossou, and Y. Dube, "Online system identification and adaptive control for PEM fuel cell maximum efficiency tracking," *IEEE Trans. Energy Convers.*, vol. 27, no. 3, pp. 580–592, Sep. 2012.

[10] M. Blanke, M. Kinnaert, J. Lunze, and M. Staroswiecki, *Diagnosis and Fault-Tolerant Control*. Berlin, Germany: Springer-Verlag, 2006.

[11] A. Rosich, R. Sarrate, and F. Nejjari, "On-line model-based fault detection and isolation for PEM fuel cell stack systems," *Appl. Math. Model.*, vol. 38, nos. 11/12, pp. 2744–2757, 2014.

[12] N. Lowery, M. Vahdati, R. Potthast, and W. Holderbaum, "Classification and fault detection methods for fuel cell monitoring and quality control," *J. Fuel Cell Sci. Technol.*, vol. 10, no. 2, pp. 1–8, 2013.

[13] A. Hernandez, D. Hissel, and R. Outbib, "Modeling and fault diagnosis of a polymer electrolyte fuel cell using electrical equivalent analysis," *IEEE Trans. Energy Convers.*, vol. 25, no. 1, pp. 148–160, Mar. 2010.

[14] W. Yang, K. Lee, S. Junker, and H. Ghezel-Ayagh, "Fuzzy fault diagnosis and accommodation system for hybrid fuel-cell/gas-turbine power plant," *IEEE Trans. Energy Convers.*, vol. 25, no. 4, pp. 1187–1194, Dec. 2010.

[15] L. Xu, J. Li, M. Ouyang, J. Hua, and X. Li, "Active fault tolerance control system of fuel cell hybrid city bus," *Int. J. Hydrogen Energy*, vol. 35, no. 22, pp. 12510–12520, 2010.

[16] D. Feroldi, "Fault diagnosis and fault tolerant control of PEM fuel cell systems," in *PEM Fuel Cells With Bio-Ethanol Processor Systems*. New York, NY, USA: Springer, 2012, pp. 185–206.

[17] I. Markovsky, "Closed-loop data-driven simulation," *Int. J. Control*, vol. 83, no. 10, pp. 2134–2139, 2010.

[18] M. Safonov and T. Tsao, "The unfalsified control concept and learning," vol. 42, no. 6, pp. 843–847, 1997. Q8

[19] M. Stefanovic and M. Safonov, *Safe Adaptive Control*. New York, NY, USA: Springer, 2011.

[20] E. Nabati and S. Engell, "Data-driven adaptive control: Making unfalsified control work better," in *Proc. 18th World Congr. Int. Fed. Autom. Control*, Milano, Italy, 2011, pp. 1285–1290.

[21] A. Neamtu and A. Stoica, "Unfalsified Control: Application to automatic flight control system design," *NCAS Bull.*, vol. 3, no. 3, pp. 103–114, 2011.

[22] A. Wolniakowski and A. Mystkowski, "Application of unfalsified control theory in controlling MAV," *Solid-State Phenom.*, vol. 198, pp. 171–175, 2013.

[23] J. van Helvoort, B. de Jager, and M. Steinbuch, "Unfalsified control using an ellipsoidal unfalsified region applied to a motion system," in *Proc. 16th World Congr. Int. Fed. Autom. Control*, Prague, Czech Republic, 2005, pp. 1–6.

[24] J. van Helvoort, B. de Jager, and M. Steinbuch, "Direct data-driven recursive controller unfalsification with analytic update," *Automatica*, vol. 43, no. 12, pp. 2034–2046, 2007.

[25] C. Kunusch and F. Castaños, "Extremum seeking algorithms for minimal hydrogen consumption in pem fuel cells," in *Proc. Amer. Control Conf.*, Washington, DC, USA, 2013, pp. 1144–1149.

[26] C. Ocampo-Martinez, R. S. Sánchez-Peña, F. Bianchi, and A. Ingimundarson, "Integrating unfalsified control and fault diagnosis for fault-tolerant control," *Int. J. Syst. Sci.*, 2014, to be published. Q9

[27] J. Zhang, G. Liu, W. Yu, and M. Ouyang, "Adaptive control of the airflow of a PEM fuel cell system," *J. Power Sources*, vol. 179, no. 2, pp. 649–659, 2008.

Fernando D. Bianchi received the B.S. and Ph.D. degrees in electronic engineering from the National University of La Plata (UNLP), Buenos Aires, Argentina, in 1999 and 2005, respectively.

From 1999 to 2006, he was a Postdoctoral Fellow at the Laboratory of Industrial Electronic, Control, and Instrumentation, UNLP. From 2006 to 2010, he was a Postdoctoral Researcher at the Technical University of Catalonia, Barcelona, Spain. In 2010, he joined the Power Electronics and Electric Power Grids Group, Catalonia Institute for Energy Research, Barcelona, as a Scientific Researcher. His main research interests include robust control and linear parameter-varying systems and their applications to the control of renewable energy conversion systems.

Carlos Ocampo-Martinez (S'97–M'12–SM'13) received the Electronic Engineering degree and the M.Sc. degree in industrial automation from the National University of Colombia, Manizales, Colombia, in 2001 and 2003, respectively, and the Ph.D. degree in control engineering from the Technical University of Catalonia, Barcelona, Spain, in 2007.

In 2008, as a Postdoctoral Fellow of the ARC Centre of Complex Dynamic Systems and Control, University of Newcastle, Australia, he was with the Spanish National Research Council, Institut de Robòtica i Informàtica Industrial, Barcelona, as a *Juan de la Cierva* Research Fellow. Since 2011, he has been an Assistant Professor at the Automatic Control Department, Technical University of Catalunya, Barcelona. His main research interests include the areas of constrained model predictive control, large-scale systems management, and nonlinear dynamics and industrial applications. Q10

Cristian Kunusch (S'03–M'10) received the B.S., M.Sc., and Ph.D. degrees in electronic engineering from the National University of La Plata, Buenos Aires, Argentina, in 2003, 2006, and 2009, respectively.

In 2010, he was appointed as a Postdoctoral Fellow of the Spanish National Research Council, Institut de Robòtica i Informàtica Industrial, Barcelona, Spain. In 2014, he joined the Electric Drives Predevelopment Team of Brose Fahrzeugteile, Würzburg, Germany, as a Senior Researcher. His main research interests include variable structure systems and their applications to the control and observation of fuel-cell-based systems and electric drives.

Ricardo S. Sánchez-Peña (S'86–M'88–SM'00) received the Electronic Engineer degree from the University of Buenos Aires (UBA), Buenos Aires, Argentina, in 1978, and the M.Sc. and Ph.D. degrees in electrical engineering from the California Institute of Technology, Pasadena, CA, USA, in 1986 and 1988, respectively.

In Argentina, he was with CITEFA, CNEA, and the space agencies CNIE **Q11** and CONAE. He collaborated with NASA in aeronautical and satellite projects, and with the German (DLR) and Brazilian (CTA/INPE) space agencies. He was **Q12** a Full Professor at UBA from 1989 to 2004, an ICREA Senior Researcher at the Universitat Politcnica de Catalunya, Barcelona, Spain, from 2005 to 2009, and a Visiting Professor/Researcher at several universities in the USA and the EU. He has consulted for ZonaTech (USA), STI, and VENG (Argentina) in aerospace **Q13** applications, and with Alstom-Ecotecnia (Spain) in wind turbine applications. Since 2009, he has been a Director of the Ph.D. Department in Engineering, Buenos Aires Institute of Technology, Buenos Aires, and is a CONICET **Q14** Principal Investigator. He has applied identification and control techniques to acoustical, mechanical, and aero and astronautical engineering, and also to type I Diabetes.

Dr. Sánchez-Peña received the Premio Consagración in Engineering by the National Academy of Exact, Physical, and Natural Sciences, Argentina, and the Group Achievement Award from NASA as a Review Board Member for the Aquarius/SAC-D satellite.

QUERIES

Q1. Author: Acronym “PEMFC” is used for two different terms in the paper. Please check.
Q2. Author: Please provide expanded form of CICYT, CONICET, PRH.
Q3. Author: Please provide expanded form of MACPERCON, CSIC.
Q4. Author: Please provide expanded form of CONICET and location details including postal code
Q5. Author: Please provide expanded form of LQR/LQG.
Q6. Author: Please provide legends for subparts in figures 5-10.
Q7. Author: Please provide journal name for reference 3.
Q8. Author: Please provide journal name for reference 18.
Q9. Author: Please update Ref. [26].
Q10. Author: Please ptovide expanded form of ARC, and location details of University of Newcastle, Australia.
Q11. Author: Please ptovide expanded form of CITEFA, CNEA, CNIE, CONAE and also provide location details.
Q12. Author: Please ptovide expanded form of DLR, CTA/INPE, ICREA.
Q13. Author: Please provide query for full location details of ZonaTech (USA), DLR, CTA/INPE, STI, VENG (Argentina), and Alstom-Ecotecnia (Spain).
Q14. Author: Please provide expanded form of CONICET and SAC-D.